Published in final edited form as:

Nature. 2021 June ; 594(7864): 553–559. doi:10.1038/s41586-021-03594-0.

Neutralizing antibody vaccine for pandemic and pre-emergent coronaviruses

Kevin O. Saunders[1,2,3,4,#], **Esther Lee**[1,5], **Robert Parks**[1,5], **David R. Martinez**[6], **Dapeng Li**[1,5], **Haiyan Chen**[1,5], **Robert J. Edwards**[1,5], **Sophie Gobeil**[1,5], **Maggie Barr**[1,5], **Katayoun Mansouri**[1,5], **S. Munir Alam**[1,5], **Laura L. Sutherland**[1,5], **Fangping Cai**[1,5], **Aja M. Sanzone**[1,5], **Madison Berry**[1,5], **Kartik Manne**[1,5], **Kevin W. Bock**[7], **Mahnaz Minai**[7], **Bianca M. Nagata**[7], **Anyway B. Kapingidza**[1,5], **Mihai Azoitei**[1,5], **Longping V. Tse**[6], **Trevor D. Scobey**[6], **Rachel L. Spreng**[1,5], **R. Wes Rountree**[1,5], **C. Todd DeMarco**[1,5], **Thomas N. Denny**[1,5], **Christopher W. Woods**[1,5,8], **Elizabeth W. Petzold**[8], **Juanjie Tang**[9], **Thomas H. Oguin III**[1,5], **Gregory D. Sempowski**[1,5], **Matthew Gagne**[10], **Daniel C. Douek**[10], **Mark A. Tomai**[11], **Christopher B. Fox**[12], **Robert Seder**[10], **Kevin Wiehe**[1,5], **Drew Weissman**[13], **Norbert Pardi**[13], **Hana Golding**[9], **Surender Khurana**[9], **Priyamvada Acharya**[1,2], **Hanne Andersen**[14], **Mark G. Lewis**[14], **Ian N. Moore**[7], **David C. Montefiori**[1,2], **Ralph S. Baric**[6], **Barton F. Haynes**[1,3,5,#]

[1]Duke Human Vaccine Institute, Duke University School of Medicine, Durham, NC 27710, USA

[2]Department of Surgery, Duke University, Durham, NC 27710, USA

[3]Department of Immunology, Duke University School of Medicine, Durham, NC 27710, USA

[4]Department of Molecular Genetics and Microbiology, Duke University School of Medicine, Durham, NC 27710, USA

[5]Department of Medicine, Duke University School of Medicine, Durham, NC 27710, USA

[6]Department of Epidemiology, University of North Carolina at Chapel Hill, Chapel Hill, NC 27599, USA

[7]Infectious Disease Pathogenesis Section, Comparative Medicine Branch, National Institute of Allergy and Infectious Diseases, National Institutes of Health, Bethesda, MD 20892, USA

[#]Correspondence: barton.haynes@duke.edu (B.F.H.) and kevin.saunders@duke.edu (K.O.S.).

AUTHOR CONTRIBUTIONS

KOS and BFH designed and managed the study, reviewed all data and wrote and edited the manuscript; DW, NP designed and produced the mRNA-LNPs; EL, AMS, FPC, and HC expressed proteins; SK, JT, HG, EL, RP, MB, THO, DRM, DCM, LVT, TDS, GDS, RSB carried out binding, virus plaque, and neutralization assays; RSB and DRM prepared recombinant live viruses encoding nLuc; DL, CTM, TD, MG, DCD designed or performed sg or genomic RNA assays; RJE, SG, PA, KatM, KarM, MA, MB, and KW performed structural or sequence analysis; SMA performed SPR; LLS, MGL, HA, RS and performed or evaluated monkey studies; KB, MM, BN, IM performed histology and immunochemistry; CWW, EWP, GDS collected, annotated, COVID-19 samples; MT selected, provided adjuvant; RWR and RLS performed statistical analyses; All authors edited and approved the manuscript.

Competing financial interests BFH and KOS have filed patents regarding the nanoparticle vaccine, MAT and 3M company have patents filed on 3M052, and CF and IDRI have filed patents on the formulation of 3M052 and alum. 3M company had no role in the execution of the study, data collection, or data interpretation. DW is named on patents that describe the use of nucleoside-modified mRNA as a platform to deliver therapeutic proteins. DW and NP are also named on a patent describing the use of nucleoside-modified mRNA in lipid nanoparticles as a vaccine platform. All other authors declare no competing interests.

Supplementary information is available for this paper

[8]Center for Applied Genomics and Precision Medicine, Duke University Medical Center, Durham, NC 27710, USA

[9]Division of Viral Products, Center for Biologics Evaluation and Research (CBER), Food and Drug Administration, Silver Spring, MD 20993, USA.

[10]Vaccine Research Center, National Institute of Allergy and Infectious Diseases (NIAID), NIH, Bethesda, MD 20892, USA

[11]Corporate Research Materials Lab, 3M Company, St. Paul, MN 55144, USA.

[12]Infectious Disease Research Institute, Seattle, WA 98102, USA

[13]Department of Medicine, University of Pennsylvania, Philadelphia, PA 19104, USA

[14]BIOQUAL, Rockville, MD 20850, USA

SUMMARY

Betacoronaviruses (betaCoVs) caused the severe acute respiratory syndrome (SARS) and Middle East Respiratory Syndrome (MERS) outbreaks, and the SARS-CoV-2 pandemic[1–4]. Vaccines that elicit protective immunity against SARS-CoV-2 and betaCoVs circulating in animals have the potential to prevent future betaCoV pandemics. Here, we show that macaque immunization with a multimeric SARS-CoV-2 receptor binding domain (RBD) nanoparticle adjuvanted with 3M-052/Alum elicited cross-neutralizing antibody (cross-nAb) responses against batCoVs, SARS-CoV-1, SARS-CoV-2, and SARS-CoV-2 variants B.1.1.7, P.1, and B.1.351. Nanoparticle vaccination resulted in a SARS-CoV-2 reciprocal geometric mean neutralization ID50 titer of 47,216, and protection against SARS-CoV-2 in macaque upper and lower respiratory tracts. Importantly, nucleoside-modified mRNA encoding a stabilized transmembrane spike or monomeric RBD also induced SARS-CoV-1 and batCoV cross-nAbs, albeit at lower titers. These results demonstrate current mRNA vaccines may provide some protection from future zoonotic betaCoV outbreaks, and provide a platform for further development of pan-betaCoV vaccines.

SARS coronavirus 1 (SARS-CoV-1), SARS coronavirus 2 (SARS-CoV-2), and MERS coronavirus (MERS-CoV) emerged from transmission events where humans were infected with bat or camel CoVs[5–8]. BetaCoVs that circulate in civets, bats, and Malayan pangolins are genetically similar to SARS-CoV-1 and SARS-CoV-2, and use human ACE2 as a receptor[5,6,9–11]. These SARS-related animal coronaviruses have the potential to be transmitted to humans[12]. Cross-nAbs capable of neutralizing multiple betaCoVs and preventing or treating betaCoV infection have been isolated from SARS-CoV-1 infected humans[13–24], providing proof-of-concept for development of betaCoV vaccines against *Sarbecoviruses*[25].

In mice, vaccine induction of cross-nAbs has been reported for CoV pseudoviruses[26,27]. However, it is unknown whether spike vaccination of primates can elicit cross-nAbs against SARS-CoV-1, bat betaCoVs, or SARS-CoV-2 escape viruses. A target of cross-nAbs is the RBD of spike[14,24,25]. One such RBD cross-nAb is antibody DH1047, which cross-neutralizes SARS-CoV-1, SARS-CoV-2 and bat CoVs[15]. RBD immunogenicity can be augmented by arraying multiple copies on nanoparticles, mimicking virus-like

particles[26–29]. Thus, we designed a 24-mer SARS-CoV-2 RBD-ferritin nanoparticle vaccine. The RBD nanoparticle was constructed by expressing recombinant SARS-CoV-2 RBD with a C-terminal sortase A donor sequence, and by expressing a 24-subunit, self-assembling protein nanoparticle *Helicobacter pylori* ferritin with an N-terminal sortase A acceptor sequence[30]. The RBD and ferritin nanoparticle were conjugated together by a sortase A reaction (Fig. 1a, Extended Data Fig. 1)[30]. Analytical size exclusion chromatography and negative stain electron microscopy confirmed that RBD was conjugated to the surface of the ferritin nanoparticle (Fig. 1a, Extended Data Fig. 1b,c). The RBD sortase A conjugated nanoparticle (RBD-scNP) bound to human ACE2, the receptor for SARS-CoV-2, and to potently neutralizing SARS-CoV-2-specific RBD antibodies (Abs) DH1041, DH1042, DH1043, DH1044, and DH1045[15] (Fig. 1b). The cross-nAb DH1047 also bound to the RBD-scNP (Fig. 1b). The RBD-scNP lacked binding to SARS-CoV-2 spike Abs that bound outside of the RBD (Fig. 1b).

Five cynomolgus macaques were immunized three times intramuscularly four weeks apart with 100 μg of RBD-scNP adjuvanted with 5 μg of the TLR7/8 agonist 3M-052 absorbed to 500 μg of alum (Fig. 1c and Extended Data Fig. 1d,e)[31]. Immunizations were well-tolerated in macaques (Extended Data Fig. 2). Immunization with RBD-scNP adjuvanted with 3M-052/Alum elicited binding IgG against SARS-CoV-2 RBD and stabilized Spike ectodomain (S-2P) (Fig. 1d), but immunization with 3M-052/Alum alone did not (Extended Data Fig. 3a,b). Boosting once maximally increased SARS-CoV-2 binding IgG titers (Fig. 1d). ACE2 competitive binding assays demonstrated the presence of ACE2-binding site Abs in the serum of vaccinated macaques (Fig. 1e). Similarly, plasma Abs blocked the binding of ACE2-binding site-focused, RBD neutralizing antibody DH1041 (Fig. 1e). Vaccine induction of nAbs was assessed against a SARS-CoV-2 pseudovirus with an aspartic acid to glycine substitution at position 614 (D614G)[32]. Two RBD-scNP immunizations induced potent serum nAbs with fifty percent inhibitory reciprocal serum dilution (ID50) neutralization titers ranging from 21,292 to 162,603 (Fig. 1f,g). We compared these nAb titers to those elicited by cynomolgus macaques immunized twice with 50 μg of lipid-encapsulated nucleoside-modified mRNA (mRNA-LNP) encoding stabilized transmembrane (TM) Spike (S-2P) that is analogous to COVID-19 vaccines authorized for emergency use (Extended Data Fig. 1f). Serum neutralization titers against SARS-CoV-2 D614G pseudovirus elicited by RBD-scNP immunization were significantly higher than titers elicited by two S-2P mRNA-LNP immunizations (Fig. 1i, group geometric mean ID50 47,216 versus 6,469, $P = 0.0079$ Exact Wilcoxon test, n=5)[33,34]. When compared to natural human infection, RBD-scNP vaccination elicited higher ID50 neutralization titers (Fig. 1j). Thus, RBD-scNP adjuvanted with 3M-052/Alum elicits significantly higher neutralizing titers in macaques compared to current vaccine platforms or natural human infection.

The SARS-CoV-2 variant B.1.1.7 or United Kingdom variant is spreading globally, and has been suggested to have higher infectivity than the Wuhan-1 strain[35,36]. B.1.351 lineage viruses are widespread in the Republic of South Africa[36–38], and along with Brazilian variant P.1 are of concern due to their neutralization-resistant phenotype mediated by mutations in the RBD at K417N, E484K, and N501Y[39]. Each of these mutations were distal to the cross-nAb DH1047 binding site owing to its long HCDR3 used to contact RBD; however, the E484K mutation was within the binding site of RBD nAb DH1041

(Fig. 2a,b)[15]. Thus, DH1041 binding to SARS-CoV-2 RBD was knocked out by the E484K mutation, but DH1047 binding to RBD was unaffected by K417N, E484K, or N501Y (Fig. 2c,d and Extended Data Fig. 3).

We determined whether RBD-scNP or mRNA-LNP immunization elicited nAbs against these particular SARS-CoV-2 variants. RBD-scNP macaque serum potently neutralized a pseudovirus bearing the D614G spike and the B.1.1.7 spike (Fig. 2d,e). Similarly, S-2P mRNA-LNP immunization elicited equivalent titers of nAbs against the B.1.1.7 and D614G variants of SARS-CoV-2, although titers were lower than RBD-scNP immunization (Fig. 2d,e). Macaque serum from RBD-scNP or mRNA-LNP immunization neutralized SARS-CoV-2 WA-1, B.1.351, and P.1 pseudoviruses, with ID80 titers being more potent for the RBD-scNP group (Fig. 2f-i). On average, the RBD-scNP group neutralization titers decreased by 3-fold against B.1.351 or P.1, whereas the mRNA-LNP group decreased by 6-fold for B.1.351 and 10-fold for P.1 based on ID50 titers (Fig. 2g,i). Additionally, we observed RBD-scNP and S-2P mRNA-LNP immune plasma IgG binding to SARS-CoV-2 S was unaffected by mutations observed in Danish minks, B.1.351, P.1, and B.1.1.7 SARS-CoV-2 strains[36,37,40] (Extended Data Fig. 3). In summary, both vaccines tested here elicited nAbs that were unaffected by the mutations in the B.1.1.7 strain. However, nAbs elicited by RBD-scNP more potently neutralized the difficult-to-neutralize B.1.351 and P.1 virus strains than nAbs elicited with S-2P mRNA-LNP immunization.

SARS-related CoVs that circulate in humans and animals remain a threat for future outbreaks[12,41,42]. Therefore, we examined neutralization of SARS-CoV-1 and SARS-related group 2b batCoV-WIV-1 and SARS-related batCoV-SHC014 viruses by immune sera from macaques vaccinated with the RBD-scNP, mRNA-LNP encoding monomeric RBD or S-2P (Extended Data Fig. 1e-g)[6,9,41,42]. After two immunizations, RBD-scNP, S-2P mRNA-LNP, and the RBD monomer mRNA-LNP elicited nAbs against SARS-CoV-1, batCoV-WIV-1, and batCoV-SHC014 (Fig. 3a, Extended Data Fig. 4). Neutralization was more potent for replication-competent SARS-CoV-2 virus compared to the other three SARS-related viruses (Fig. 3a, Extended Data Fig. 4), with neutralization titers varying up to 4-fold within the RBD-scNP group (Extended Data Fig. 4). Overall, RBD-scNP immunization elicited the highest neutralization titers (Fig. 3a, Extended Data Fig. 4). Small increases in neutralization potency were gained by boosting a third time with the RBD-scNP (Fig. 3b). Moreover, RBD-scNP immunization elicited cross-reactive plasma IgG against SARS-CoV-2, SARS-CoV-1, batCoV-RaTG13, batCoV-SHC014, pangolin CoV-GXP4L Spike proteins (Fig. 3c and Extended Data Fig. 5a,c). Binding antibody titers were high for these spikes, even in instances where neutralization titers were low suggesting non-nAbs contributed to binding titers. RBD-scNP immune plasma IgG did not bind spike from the four endemic human CoVs or MERS-CoV (Extended Data Fig. 5a,c). The lack of binding by plasma IgG to these latter five S ectodomains was consistent with RBD sequence divergence among groups 1, 2a, 2b and 2c coronaviruses (Fig. 3f and Extended Data Fig. 6-7). The SARS-CoV-2 spike induced cross-nAbs against multiple group 2b SARS-related betaCoVs, with the highest titers induced by RBD-scNP.

Immune sera from RBD-scNP-immunized macaques exhibited a similar cross-neutralizing profile as the cross-nAb DH1047. DH1047 bound with <0.02 nM affinity to monomeric

SARS-CoV-2 RBD (Extended Data Fig. 5b), and bound the RBD-scNP (Fig. 1b). The cross-reactive DH1047 epitope is adjacent to the N-terminus of the ACE2-binding site, distinguishing it from dominant ACE2 binding site-focused nAbs such as DH1041 (Fig. 3d)[15], and it has high group 2b sequence conservation (Fig. 3e). Overall RBD sequences within betaCoV groups are more conserved than sequences from different groups (Fig. 3f and Extended Data Fig. 6-7). The presence of DH1047-like antibodies was determined with DH1047 blocking assays. Plasma from all RBD-scNP-immunized macaques blocked the binding of ACE2 and DH1047 to SARS-CoV-2 S-2P ectodomain (Fig. 3g and Extended Data Fig. 5d). The DH1047-blocking antibodies were cross-reactive as they also potently blocked DH1047 binding to batCoV-SHC014 S-2P (Fig. 3g). RBD-scNP immunization elicited higher magnitudes of DH1047 blocking Abs than S-2P mRNA-LNP immunization of macaques, Pfizer/BNT162b2 mRNA-LNP immunization of humans, or SARS-CoV-2 human infection (Fig. 3h and Extended Data Fig. 5d). ACE2 blocking was high in all groups (Fig. 3h). While 5 of 5 RBD-scNP-vaccinated macaques exhibited potent DH1047 serum blocking activity, 3 of 4 immunized humans and 9 of 22 of COVID-19 convalescent humans had detectable serum DH1047 blocking activity (Fig. 3h). Thus, the DH1047-like antibody response was subdominant in infected or immunized humans and S-2P mRNA-LNP-immunized macaques, but was a dominant antibody response to RBD-scNP vaccination.

To determine vaccine protection against coronavirus infection, we challenged RBD-scNP-vaccinated and S-2P mRNA-LNP primed/RBD-scNP boosted monkeys with 10^5 plaque forming units of SARS-CoV-2 virus via intratracheal and intranasal routes after their last boost (Fig. 4a). NAbs were detectable in all macaques 2 weeks after the final immunization (Fig. 3b and Extended Data Fig. 4b,c). Bronchoalveolar lavage (BAL) fluid was collected 2 days post challenge (Fig. 4a). Infectious SARS-CoV-2 was detectable in BAL fluid from 5 of 6 unimmunized macaques, and undetectable in all RBD-scNP and S-2P mRNA-LNP/RBD-scNP-immunized macaques (Fig. 4b). Copies of Envelope (E) and Nucleocapsid (N) subgenomic RNA in fluid from nasal swabs and bronchoalveolar lavage (BAL) two and four days after challenge was used to quantify SARS-CoV-2 replication (Fig. 4a). On day 2 after challenge, unimmunized macaques had an average of $1.3x10^5$ and $1.2x10^4$ copies/mL of E sgRNA in the nasal swab and BAL fluids, respectively (Fig. 4c,d). In contrast, RBD-scNP-vaccinated monkeys and 4 of 5 S-2P mRNA-LNP monkeys had undetectable levels of E sgRNA in the upper and lower respiratory tract (Fig. 4c,d). We sampled monkeys again 2 days later, and found no detectable E sgRNA in any vaccinated monkey BAL or nasal swab samples (Fig. 4b,c). Similarly, all RBD-scNP-vaccinated macaque had undetectable N sgRNA in BAL and the nasal swab fluid, except one macaque that had 234 copies/mL of N sgRNA detected on day 2 in nasal swab fluid (Fig. 4e,f). Virus replication was undetectable in this macaque by the fourth day after challenge (Fig. 4e). Additionally, all but one mRNA-LNP/RBD-scNP-immunized macaque had undetectable N sgRNA in BAL or nasal swab samples (Fig. 4e,f). Moreover, SARS-CoV-2 nucleocapsid antigen was undetectable in the lung tissue of all vaccinated macaques, but was detected in all control macaques (Fig. 4g and Extended Data Fig. 8). Hematoxylin and eosin staining of lung tissue showed a reduction in inflammation in immunized macaques compared to control macaques (Extended Data Fig. 8 and Extended Data Table 1).

Finally, mucosal immunity to SARS-CoV-2 were examined when possible both before and after SARS-CoV-2 challenge (Extended Data Fig. 9). IgG from concentrated BAL bound to spike and blocked ACE-2, DH1041, and DH1047 binding to spike (Extended Data Fig. 9b-d). Each response was higher in the BAL from monkeys immunized three times with RBD-scNP compared to monkeys immunized two times with S-2P mRNA-LNP and boosted once with RBD-scNP, although the BAL was collected from each group at different timepoints. Unconcentrated nasal wash samples from monkeys immunized with either RBD-scNPs or S-2P mRNA-LNP prime/RBD-scNP boost showed similar low levels of spike-binding IgG post challenge (Extended Data Fig. 9e). Nonetheless, RBD-scNP-immunization elicited RBD-specific mucosal antibodies.

As three coronavirus epidemics have occurred in the past 20 years, there is a need to develop effective pancoronavirus vaccines prior to the next pandemic[25]. The epitopes of betaCoV cross-nAbs, such as DH1047, provide clear targets for vaccines aiming to protect against multiple CoVs[13–15,43]. We have shown that immunization with RBD-scNP adjuvanted with a toll-like receptor agonist 3M-052, and spike mRNA-LNP to a lesser extent, induces cross-nAbs against multiple SARS-related human and bat betaCoVs in primates. These results demonstrate that SARS-CoV-2 vaccination with either the RBD-scNP or spike mRNA-LNP vaccines similar to those authorized for use in humans, will likely elicit cross-nAbs with the potential to prevent future group 2b betaCoV spillover from bats to humans [12,26].

The emergence of SARS-CoV-2 neutralization-resistant and highly infectious variants continues to be a concern for vaccine efficacy. RBD-scNP and SARS-CoV-2 spike mRNA-LNP immunizations elicited SARS-CoV-2 nAbs against SARS-CoV-2 D614G, B.1.1.7 , P.1, and B.1.351 strains. The nAbs elicited by RBD-scNP and S-2P mRNA-LNP were of different specificities since RBD-scNP-induced nAbs showed a smaller reduction in neutralization potency across the different variants compared to S-2P mRNA-LNP immune sera. Our results are consistent with the demonstration that current COVID-19 vaccines have reduced efficacy against the B.1.351 SARS-CoV-2 variant[44–49].

The RBD-scNP vaccine is a promising platform for pancoronavirus vaccine development for the following reasons. The RBD-scNP vaccine induced apparent sterilizing immunity in the upper respiratory tract, which has not been routinely achieved with SARS-CoV-2 vaccination in macaques [50,51]. Additionally, the extraordinarily high neutralization titers achieved by RBD-scNP vaccination bode well for an extended duration of protection. Despite the induction of high levels of antibody we observed no evidence of increased immunopathology, inflammatory cytokines or virus replication indicative vaccine-elicited antibody-dependent enhancement. Lack of *in vivo* infection enhancement is consistent with studies using SARS-CoV-2 monoclonal Abs[15]. 3M-052 adsorbed to Alum is in clinical testing (NCT04177355) generating a potential translational pathway for RBD-scNP adjuvanted with 3M-052. The RBD-scNP/3M-052 vaccine represents a platform for producing pancoronavirus vaccines that could prevent, rapidly temper, or extinguish the next spillover of a coronavirus into humans.

METHODS

Animals, immunizations, and human samples.

Rhesus and cynomolgus macaques were housed and treated in AAALAC-accredited institutions. The study protocol and all veterinarian procedures were approved by the Bioqual IACUC per a memorandum of understanding with the Duke IACUC, and were performed based on standard operating procedures. Nucleoside-modified messenger RNA encapsulated in lipid nanoparticles (mRNA-LNP) was prepared as previously stated [52,53]. Rhesus macaques (n=8 macaques) were immunized intramuscularly with 50μg of mRNA-LNP encoding the receptor binding domain (RBD) monomer. Cynomolgus macaques (n=5 macaques) were immunized twice with 50μg of mRNA-LNP encoding the transmembrane Spike protein stabilized with K986P and V987P mutations and boosted once with 100 μg of RBD-scNP adjuvanted with 5 μg of 3M-052 aqueous formulation (AF) admixed with 500 μg of Alum in PBS. An additional group of cynomolgus macaques (n=5 macaques) were immunized in the right and left quadriceps with 100 μg of RBD-scNP adjuvanted with 5 μg of 3M-052 aqueous formulation (AF) admixed with 500 μg of Alum in PBS [31]. The mixture for immunization consisted of 250 μL of RBD-scNP mixed with 250 μL of 0.02 mg/ml 3M-052, 2 mg/ml Alum. Group sizes were selected such that statistical significance could be reached with between group nonparametric statistical comparisons. Macaques were on average 8 or 9 years old and ranged from 2.75 to 8 kg in body weight. Male and females per group were balanced when macaque availability permitted it. Studies were performed unblinded. Animals were evaluated by Bioqual veterinary staff before during and after immunizations. In the animals studied, CBCs and chemistries were obtained throughout the immunization regimen and no significant abnormalities were noted. Of the 10 cynomolgus macaques, there were no adverse events reported at injection sites. Over the course of the study, 2 cynomolgus macaques experienced slight weight loss. Two cynomolgus macaques showed a single incidence of poor appetite, with one additional cynomolgus macaque showing poor appetite intermittently throughout the study. Additionally, one macaque presented with an infected lymph node biopsy site that responded to appropriate veterinary treatment. Biospecimens before challenge, 2 days post-challenge, and 4 days post challenge were collected as described previously [15]. Human samples were obtained with informed consent. All recruitment, sample collection, and experimental procedures using human samples have been approved by the Duke Institutional Review Board.

SARS-CoV-2 intranasal and intratracheal challenge.

All animals were challenged at week 11 (3 weeks after last vaccination) through combined intratracheal (IT, 3.0 mL) and intranasal (IN, 0.5 mL per nostril) inoculation with an infectious dose of 105 PFU of SARS-CoV-2 (2019-nCoV/USA-WA1/2020). The stock was generated at BIOQUAL (lot# 030120–1030, 3.31 x 10^5 PFU/mL) from a p4 seed stock obtained from BEI Resources (NR-52281). The stock underwent deep sequencing to confirm homology with the WA1/2020 isolate. Virus was stored at -80°C prior to use, thawed by hand and placed immediately on wet ice. Stock was diluted to 2.5x10^4 PFU/mL in PBS and vortexed gently for 5 seconds prior to inoculation. Nasal swabs, bronchoalveolar lavage (BAL), plasma, and serum samples were collected seven days before, two days after, and four days after challenge. Unimmunized control cynomolgus macaques (N=5)

comprised were macaques that had been infused with a 10 mg/kg of a control antibody (CH65) and then 3 days later challenged with the same challenge dose and stock of SARS-CoV-2 as used in RBD-scNP-immunized macaques or 2P spike protein mRNA-LNP/RBD-scNP-immunized macaques. Protection from SARS-CoV-2 infection was determined by quantitative PCR of SARS-CoV-2 subgenomic Envelope (E) and the more sensitive Nucleocapsid (N) RNA (E or N sgRNA) [39] as stated below.

SARS-CoV-2 protein production.

The CoV ectodomain constructs were produced and purified as described previously [54]. The Spike (S) ectodomain was stabilized by the introduction of 2 prolines at amino acid positions 986 and 987 and referred to as S-2P. Plasmids encoding Spike-2P and HexaPro [55] were transiently transfected in FreeStyle 293 cells (Thermo Fisher) using Turbo293 (SpeedBiosystems) or 293Fectin (ThermoFisher). All cells were tested monthly for mycoplasma. The constructs contained an HRV 3C-cleavable C-terminal twinStrepTagII-8xHis tag. On day 6, cell-free culture supernatant was generated by centrifugation of the culture and filtering through a 0.8 um filter. Protein was purified from filtered cell culture supernatants by StrepTactin resin (IBA) and by size exclusion chromatography using Superose 6 column (GE Healthcare) in 10 mM Tris pH8,150 mM NaCl or 2 mM Tris pH 8, 200 mM NaCl, 0.02% NaN_3. ACE-2-Fc was expressed by transient transfection of Freestyle 293-F cells[54]. ACE2-Fc was purified from cell culture supernatant by HiTrap protein A column chromatography and Superdex200 size exclusion chromatography in 10 mM Tris pH8,150 mM NaCl. SARS-CoV-2 NTD was produced as previously described [56]. SARS-CoV-2 fusion peptide was synthesized (GenScript).

Sortase A conjugation of SARS-CoV-2 RBD to *H. pylori* ferritin nanoparticles.

Wuhan strain SARS-CoV-2 RBD was expressed with sortase A donor sequence LPETGG encoded at its c-terminus. C-terminal to the sortase A donor sequence was an HRV-3C cleavage site, 8X his tag, and a twin StrepTagII (IBA). The SARS-CoV-2 RBD was expressed in Freestyle293 cells and purified by StrepTactin affinity chromatography (IBA) and superdex200 size exclusion chromatography as stated above. *H. pylori* ferritin particles were expressed with a pentaglycine sortase A acceptor sequence encoded at its N-terminus of each subunit. For affinity purification of ferritin particles, 6XHis tags were appended C-terminal to a HRV3C cleavage site. Ferritin particles with a sortase A N-terminal tag were buffer exchanged into 50mM Tris, 150mM NaCI, 5mM CaCI2, pH7.5. 180 μM SARS-CoV-2 RBD was mixed with 120 μM of ferritin subunits and incubated with 100 μM of sortase A overnight at room temperature. Following incubation conjugated particles were isolated from free ferritin or free RBD by size exclusion chromatography using a Superose6 16/60 column.

Biolayer interferometry binding assays.

Binding was measured using an OctetRed 96 (ForteBio). Anti-human IgG capture (AHC) sensor tips (Forte Bio) were hydrated for at least 10 minutes in PBS. ACE2 and monoclonal Abs were diluted to 20 μg/mL in PBS and placed in black 96-well assay plate. The influenza antibody CH65 was used as the background reference antibody. The RBD nanoparticle was diluted to 50 μg/mL in PBS and added to the assay plate. Sensor tips were loaded

with antibody for 120 s. Subsequently, the sensor tips were washed for 60 s in PBS to removed unbound antibody. The sensor tips were incubated in a fresh well of PBS to establish baseline reading before being dipped into RBD-scNP to allow association for 400 s. To measure dissociation of the antibody-RBD-scNP complex, the tip was incubated in PBS for 600 s. At the end of dissociation, the tip was ejected and a new tip was attached to load another antibody. The data was analyzed with Data Analysis HT v12 (ForteBio). Background binding observed with CH65 was subtracted from all values. All binding curves were aligned to the start of association. The binding response at the end of the 400 s association phase was plotted in GraphPad Prism v9.0.

Surface plasmon resonance (SPR) assays.

SPR measurements of DH1047 antigen binding fragment (Fab) binding to monomeric SARS-CoV-2 RBD proteins were performed in HBS-EP+ running buffer using a Biacore S200 instrument (Cytiva). Assays were performed in the DHVI BIA Core Facility. The RBD was first captured via its twin-StrepTagII onto a Series S Streptavidin chip to a level of 300–400 resonance units (RU). The antibody Fabs were injected at 0.5 to 500 nM over the captured S proteins using the single cycle kinetics injection mode at a flow rate of 50 μL/min. Fab association occurred for 180 s followed by a dissociation of 360 seconds after the end of the association phase. At the end of the dissociation phase the RBD was regenerated with a 30 s injection of glycine pH1.5. Binding values were analyzed with Biacore S200 Evaluation software (Cytiva). References included blank streptavidin surface along with blank buffer binding and was subtracted from DH1047 values to account for signal drift and non-specific protein binding. A 1:1 Langmuir model with a local Rmax was used for curve fitting. Binding rates and constants were derived from the curve. Representative results from two independent experiments are shown.

BAL plaque assay.

SARS-CoV-2 Plaque assays were performed in the Duke Regional Biocontainment BSL3 Laboratory (Durham, NC) as previously described [57]. Serial dilutions of BAL fluid-were incubated with Vero E6 cells in a standard plaque assay [58,59]. BAL and cells were incubated at 37°C, 5% CO2 for 1 hour. At the end of the incubation, 1 mL of a viscous overlay (1:1 2X DMEM and 1.2% methylcellulose) was added to each well. Plates are incubated for 4 days. After fixation, staining and washing, plates were dried and plaques from each dilution of BAL sample were counted. Data are reported as plaque forming units per milliliter of BAL fluid. Samples were collected in virus transport media from six unimmunized, SARS-CoV-2-challenged macaques for comparison to vaccinated macaques.

SARS-CoV-2 pseudovirus neutralization.

For SARS-CoV-2 D614G and SARS-CoV-2 B.1.1.7 pseudovirus neutralization assays, neutralization of SARS-CoV-2 Spike-pseudotyped virus was performed by adapting an infection assay described previously with lentiviral vectors and infection in 293T/ACE2.MF (the cell line was kindly provided by Drs. Mike Farzan and Huihui Mu at Scripps). Cells were maintained in DMEM containing 10% FBS and 50 μg/ml gentamicin. An expression plasmid encoding codon-optimized full-length spike of the Wuhan-1 strain (VRC7480), was provided by Drs. Barney Graham and Kizzmekia Corbett at the Vaccine Research Center,

National Institutes of Health (USA). The D614G mutation was introduced into VRC7480 by site-directed mutagenesis using the QuikChange Lightning Site-Directed Mutagenesis Kit from Agilent Technologies (Catalog # 210518). The mutation was confirmed by full-length spike gene sequencing. Pseudovirions were produced in HEK 293T/17 cells (ATCC cat. no. CRL-11268) by transfection using Fugene 6 (Promega, Catalog #E2692). Pseudovirions for 293T/ACE2 infection were produced by co-transfection with a lentiviral backbone (pCMV ΔR8.2) and firefly luciferase reporter gene (pHR' CMV Luc) [60]. Culture supernatants from transfections were clarified of cells by low-speed centrifugation and filtration (0.45 μm filter) and stored in 1 ml aliquots at -80 °C.

For 293T/ACE2 neutralization assays, a pre-titrated dose of virus was incubated with 8 serial 3-fold or 5-fold dilutions of mAbs in duplicate in a total volume of 150 μL for 1 h at 37 °C in 96-well flat-bottom poly-L-lysine-coated culture plates (Corning Biocoat). SARS-CoV-2 RBD nAb DH1043 spiked into normal human serum was used as a positive control. Cells were suspended using TrypLE express enzyme solution (Thermo Fisher Scientific) and immediately added to all wells (10,000 cells in 100 μL of growth medium per well). One set of 8 control wells received cells + virus (virus control) and another set of 8 wells received cells only (background control). After 66–72 h of incubation, medium was removed by gentle aspiration and 30 μL of Promega 1x lysis buffer was added to all wells. After a 10-minute incubation at room temperature, 100 μl of Bright-Glo luciferase reagent was added to all wells. After 1–2 minutes, 110 μl of the cell lysate was transferred to a black/white plate (Perkin-Elmer). Luminescence was measured using a PerkinElmer Life Sciences, Model Victor2 luminometer.

To make WA-1, P.1, and B.1.351 SARS-CoV-2 pseudoviruses, human codon-optimized cDNA encoding SARS-CoV-2 S glycoproteins of various strains were synthesized by GenScript and cloned into eukaryotic cell expression vector pcDNA 3.1 between the *BamH*I and *Xho*I sites. Pseudovirions were produced by co-transfection of Lenti-X 293T cells with psPAX2(gag/pol), pTrip-luc lentiviral vector and pcDNA 3.1 SARS-CoV-2-spike-deltaC19, using Lipofectamine 3000. The supernatants were harvested at 48h post transfection and filtered through 0.45-μm membranes and titrated using 293-ACE2-TMPRSS2 cells (HEK293T cells that express ACE2 protein).

For the neutralization assay, 50 μL of SARS-CoV-2 S pseudovirions were pre-incubated with an equal volume of medium containing serum at varying dilutions at room temperature for 1 h, then virus-antibody mixtures were added to 293T-ACE2 (WA-1 and B.1.351 assays) or 293-ACE2-TMPRSS2 (WA-1 and P.1 assays) cells in a 96-well plate. After a 3 h incubation, the inoculum was replaced with fresh medium. Cells were lysed 24 h later, and luciferase activity was measured using luciferin. Controls included cell only control, virus without any antibody control and positive control sera. Neutralization titers are the serum dilution (ID50/ID80) at which relative luminescence units (RLU) were reduced by 50% and 80% compared to virus control wells after subtraction of background RLUs.

Live virus neutralization assays.

Full-length SARS-CoV-2, SARS-CoV, WIV-1, and RsSHC014 viruses were designed to express nanoluciferase (nLuc) and were recovered via reverse genetics as described

previously [61–63]. Virus titers were measured in Vero E6 USAMRIID cells, as defined by plaque forming units (PFU) per ml, in a 6-well plate format in quadruplicate biological replicates for accuracy. For the 96-well neutralization assay, Vero E6 USAMRID cells were plated at 20,000 cells per well the day prior in clear bottom black walled plates. Cells were inspected to ensure confluency on the day of assay. Serum samples were tested at a starting dilution of 1:20 and were serially diluted 3-fold up to nine dilution spots. Serially diluted serum samples were mixed in equal volume with diluted virus. Antibody-virus and virus only mixtures were then incubated at 37°C with 5% CO_2 for one hour. Following incubation, serially diluted sera and virus only controls were added in duplicate to the cells at 75 PFU at 37°C with 5% CO_2. After 24 hours, cells were lysed, and luciferase activity was measured via Nano-Glo Luciferase Assay System (Promega) according to the manufacturer specifications. Luminescence was measured by a Spectramax M3 plate reader (Molecular Devices, San Jose, CA). Virus neutralization titers were defined as the sample dilution at which a 50% reduction in RLU was observed relative to the average of the virus control wells. Prebleed or unimmunized control macaque values were subtracted from WIV-1 neutralization titers, but all other viruses were not background subtracted.

Biocontainment and biosafety.

All work described here was performed with approved standard operating procedures for SARS-CoV-2 in a biosafety level 3 (BSL-3) facility conforming to requirements recommended in the Microbiological and Biomedical Laboratories, by the U.S. Department of Health and Human Service, the U.S. Public Health Service, and the U.S. Center for Disease Control and Prevention (CDC), and the National Institutes of Health (NIH).

Plasma and mucosal IgG blocking of ACE2 binding.

For ACE2 blocking assays, plates were coated with 2 μg/mL recombinant ACE2 protein, then washed and blocked with 3% BSA in 1X PBS. While assay plates blocked, purified antibodies were diluted as stated above, only in 1% BSA with 0.05% Tween-20. In a separate dilution plate Spike-2P protein was mixed with the antibodies at a final concentration equal to the EC50 at which spike binds to ACE2 protein. The mixture was allowed to incubate at room temperature for 1 hour. Blocked assay plates were then washed and the antibody-spike mixture was added to the assay plates for a period of 1 hour at room temperature. Plates were washed and a polyclonal rabbit serum against the same spike protein (nCoV-1 nCoV-2P.293F) was added for 1 hour, washed and detected with goat anti rabbit-HRP (Abcam cat# ab97080) followed by TMB substrate. The extent to which antibodies were able to block the binding spike protein to ACE2 was determined by comparing the OD of antibody samples at 450 nm to the OD of samples containing spike protein only with no antibody. The following formula was used to calculate percent blocking: blocking% = (100 - (OD sample/OD of spike only)*100).

Plasma and mucosal IgG blocking of RBD monoclonal antibody binding.

Blocking assays for DH1041 and DH1047 were performed as stated above for ACE2, except plates were coated with either DH1041 or DH1047 instead of ACE2.

Plasma and mucosal IgG ELISA binding assays.

For ELISA binding assays of Coronavirus Spike antibodies, the antigen panel included SARS-CoV-2 Spike S1+S2 ectodomain (ECD) (SINO, Catalog # 40589-V08B1), SARS-CoV-2 Spike-2P [54], SARS-CoV-2 Spike S2 ECD (SINO, Catalog # 40590-V08B), SARS-CoV-2 Spike RBD from insect cell sf9 (SINO, Catalog # 40592-V08B), SARS-CoV-2 Spike RBD from mammalian cell 293 (SINO, Catalog # 40592- V08H), SARS-CoV-2 Spike NTD-Biotin, SARS-CoV Spike Protein DeltaTM (BEI, Catalog # NR-722), SARS-CoV WH20 Spike RBD (SINO, Catalog # 40150-V08B2), SARS-CoV WH20 Spike S1 (SINO, Catalog #40150-V08B1), SARS-CoV-1 RBD, MERS-CoV Spike S1+S2 (SINO, Catalog # 40069-V08B), MERS-CoV Spike S1 (SINO, Catalog #40069-V08B1), MERS-CoV Spike S2 (SINO, Catalog #40070-V08B), MERS-CoV Spike RBD (SINO, Catalog #40071-V08B1), MERS-CoV Spike RBD.

For binding ELISA, 384-well ELISA plates were coated with 2 μg/mL of antigens in 0.1 M sodium bicarbonate overnight at 4°C. Plates were washed with PBS + 0.05% Tween 20 and blocked with assay diluent (PBS containing 4% (w/v) whey protein, 15% Normal Goat Serum, 0.5% Tween-20, and 0.05% Sodium Azide) at room temperature for 1 hour. Plasma or mucosal fluid were serially diluted three-fold in superblock starting at a 1:30 dilution. Nasal was fluid started from neat and diluted 1:30, whereas BAL fluid was concentrated 10-fold. To concentrate BAL, individual BAL aliquots from the same animal and same time point were pooled in 3KDa MWCO ultrafiltration tubes (Sartorious #VS2091). Pooled BAL was concentrated by centrifugation at 3500 rpm for 30 minutes or until volume was reduced by a factor of 10. Pool was then aliquoted and frozen at -80°C until its use in an assay. Purified mAb samples were diluted to 100 μg/mL and then serially diluted 3-fold in assay diluent. Samples were added to the antigen-coated plates, and incubated for 1 h, followed by washes with PBS-0.1% Tween 20. HRP-conjugated goat anti-human IgG secondary Ab or mouse anti-rhesus IgG secondary antibody (SouthernBiotech, catalog #2040–05) was diluted to 1:10,000 and incubated at room temperature for 1 hour. These plates were washed four times and developed with tetramethylbenzidine substrate (SureBlue Reserve- KPL). The reaction was stopped with 1 M HCl, and optical density at 450 nm (OD_{450}) was determined.

Subgenomic RNA real time PCR quantification.

The assay for SARS-CoV-2 quantitative Polymerase Chain Reaction (qPCR) detects total RNA using the WHO primer/probe set E_Sarbeco (Charité/Berlin). A QIAsymphony SP (Qiagen, Hilden, Germany) automated sample preparation platform along with a virus/pathogen DSP midi kit and the *complex800* protocol were used to extract viral RNA from 800 μL of pooled samples. A reverse primer specific to the envelope gene of SARS-CoV-2 (5'-ATA TTG CAG CAG TAC GCA CAC A-3') was annealed to the extracted RNA and then reverse transcribed into cDNA using SuperScript™ III Reverse Transcriptase (Thermo Fisher Scientific, Waltham, MA) along with RNAse Out (Thermo Fisher Scientific, Waltham, MA). The resulting cDNA was treated with RNase H (Thermo Fisher Scientific, Waltham, MA) and then added to a custom 4x TaqMan™ Gene Expression Master Mix (Thermo Fisher Scientific, Waltham, MA) containing primers and a fluorescently labeled hydrolysis probe specific for the envelope gene of SARS-CoV-2 (forward primer 5'-ACA

GGT ACG TTA ATA GTT AAT AGC GT-3', reverse primer 5'-ATA TTG CAG CAG TAC GCA CAC A-3', probe 5'-6FAM/AC ACT AGC C/ZEN/A TCC TTA CTG CGC TTC G/IABkFQ-3'). The qPCR was carried out on a QuantStudio 3 Real-Time PCR System (Thermo Fisher Scientific, Waltham, MA) using the following thermal cycler parameters: heat to 50°C, hold for 2 min, heat to 95°C, hold for 10 min, then the following parameters are repeated for 50 cycles: heat to 95°C, hold for 15 seconds, cool to 60°C and hold for 1 minute. SARS-CoV-2 RNA copies per reaction were interpolated using quantification cycle data and a serial dilution of a highly characterized custom DNA plasmid containing the SARS-CoV-2 envelope gene sequence. Mean RNA copies per milliliter were then calculated by applying the assay dilution factor (DF=11.7). The limit of detection (LOD) for this assay is approximately 62 RNA copies per mL of sample.

Recombinant IgG production.

Expi293-F cells were diluted to 2.5E6 cells/mL on the day of transfection. Cells were co-transfected with Expifectamine and heavy and light chain expression plasmids. Enhancers were added 16h after transfection. On day 5, the cell culture was cleared of cells by centrifugation, filtered, and incubated with protein A beads overnight. The next day the protein A resin was washed with Tris buffered saline and then added to a 25 mL column. The resin was washed again and then glacial acetic acid was used to elute antibody off of the protein A resin. The pH of the solution was neutralized with 1M Tris pH8. The antibody was buffer exchanged into 25 mM sodium citrate pH6 supplemented with 150 mM NaCl, 0.2 μm filtered, and frozen at -80°C.

Negative stain electron microscopy.

The RBD nanoparticle protein at ~1–5 mg/ml concentration that had been flash frozen and stored at -80 °C was thawed in an aluminum block at 37 °C for 5 minutes; then 1–4 μL of RBD nanoparticle was diluted to a final concentration of 0.1 mg/ml into room-temperature buffer containing 150 mM NaCl, 20 mM HEPES pH 7.4, 5% glycerol, and 7.5 mM glutaraldehyde. After 5 minutes cross-linking, excess glutaraldehyde was quenched by adding sufficient 1 M Tris pH 7.4 stock to give a final concentration of 75 mM Tris and incubated for 5 minutes. For negative stain, carbon-coated grids (EMS, CF300-cu-UL) were glow-discharged for 20s at 15 mA, after which a 5-μl drop of quenched sample was incubated on the grid for 10–15 s, blotted, and then stained with 2% uranyl formate. After air drying grids were imaged with a Philips EM420 electron microscope operated at 120 kV, at 82,000× magnification and images captured with a 2k x 2k CCD camera at a pixel size of 4.02 Å.

Processing of negative stain images.

The RELION 3.0 program was used for all negative stain image processing. Images were imported, CTF-corrected with CTFFIND, and particles were picked using a spike template from previous 2D class averages of spike alone. Extracted particle stacks were subjected to 2–3 rounds of 2D class averaging and selection to discard junk particles and background picks. Cleaned particle stacks were then subjected to 3D classification using a starting model created from a bare spike model, PDB 6vsb, low-pass filtered to 30 Å. Classes that showed

clearly-defined Fabs were selected for final refinements followed by automatic filtering and B-factor sharpening with the default Relion post-processing parameters.

Betacoronavirus sequence analysis.

Heatmaps of amino acid sequence similarity were computed for a representative set of betacoronaviruses using the ComplexHeatmap package in R. Briefly, 1408 betacoronavirus sequences were retrieved from NCBI Genbank, aligned to the Wuhan-1 spike protein sequence, and trimmed to the aligned region. The 1408 spike sequences were then clustered using USEARCH [64] with a sequence identity threshold of 0.90 resulting in 52 clusters. We sampled one sequence from each cluster to generate a representative set of sequences. Five betacoronavirus sequences of interest not originally included in the clustered set were added: SARS-CoV-2, GXP4L, batCoV-RaTG13, batCoV-SHC014, batCoV-WIV-1. This resulted in a set of 57 representative spike sequences. Pairs of spike amino acid sequences were aligned using a global alignment and the BLOSUM62 scoring matrix. For RBD and NTD domain alignments, spike sequences were aligned to the Wuhan 1 spike protein RBD region (residues 330–521) and NTD region (residues 27–292), respectively, and trimmed to the aligned region. Phylogenetic tree construction of RBD sequences was performed with Geneious Prime 2020.1.2 using the Neighbor Joining method and default parameters. To map group 2b betaCoV sequence conservation onto the RBD structure, group 2b spike sequences were retrieved from Genbank and clustered using USEARCH [64] with a sequence identity threshold of 0.99 resulting in 39 clusters. For clusters of size >5, 5 spike sequences were randomly downsampled from each cluster. The resulting set of 73 sequences was aligned using MAFFT [65]. Conservation scores for each position in the multiple sequence alignment were calculated using the trident scoring method [66] and computed using the MstatX program (https://github.com/gcollet/MstatX). The conservation scores were then mapped to the RBD domain coordinates (PDB: 7LD1) and images rendered with PyMol version 2.3.5.

Histopathology.

Lung specimen from macaques were fixed in 10% neutral-buffered formalin, processed, and blocked in paraffin for histology analyses. All tissues were sectioned at 5 μm and stained with hematoxylin-eosin (H&E) for to assess histopathology. Stained sections were evaluated by a board-certified veterinary pathologist in a blinded manner. Sections were examined under light microscopy using an Olympus BX51 microscope and photographs were taken using an Olympus DP73 camera.

Immunohistochemistry (IHC).

Staining for SARS-CoV-2 nucleocapsid antigen was performed by the Bond RX automated system with the Polymer Define Detection System (Leica) following the manufacturer's protocol. Tissue sections were dewaxed with Bond Dewaxing Solution (Leica) at 72°C for 30 min, then subsequently rehydrated with graded alcohol washes and 1x Immuno Wash (StatLab). Heat-induced epitope retrieval (HIER) was performed using Epitope Retrieval Solution 1 (Leica) and by heating the tissue section to 100°C for 20 min. A peroxide block (Leica) was applied for 5 min to quench endogenous peroxidase activity prior to applying the SARS-CoV-2 nucleocapsid antibody (1:2000, GeneTex, GTX135357).

Antibodies were diluted in Background Reducing Antibody Diluent (Agilent). The tissue was subsequently incubated with an anti-rabbit HRP polymer (Leica) and colorized with 3,3'-Diaminobenzidine (DAB) chromogen for 10 min. Slides were counterstained with hematoxylin.

Reagent authentication.

Cell lines were received with a certificate of authentication certifying their identity. Cell identity was also confirmed by visualizing cell morphology and using flow cytometry to detect cell surface proteins. Cells were confirmed to be free of mycoplasma with monthly testing.

Statistics Analysis.

Data were plotted using Prism GraphPad 9.0. Wilcoxon rank sum exact test was performed to compare differences between groups with p-value < 0.05 considered significant using SAS 9.4 (SAS Institute, Cary, NC). No adjustments were made to the p-values for multiple comparisons. IC50 and IC80 values were calculated using R statistical software (version 4.0.0; R Foundation for Statistical Computing, Vienna, Austria). The R package 'nplr' was used to fit 4-Parameter Logistic (4-PL) regression curves to the average values from duplicate experiments, and these fits were used to estimate the concentrations corresponding to 50% and 80% neutralization.

Data Availability Statement.

The authors declare that the data supporting the findings of this study are available within the main and supplemental figures. All data is available in the Source Data File.

Extended Data

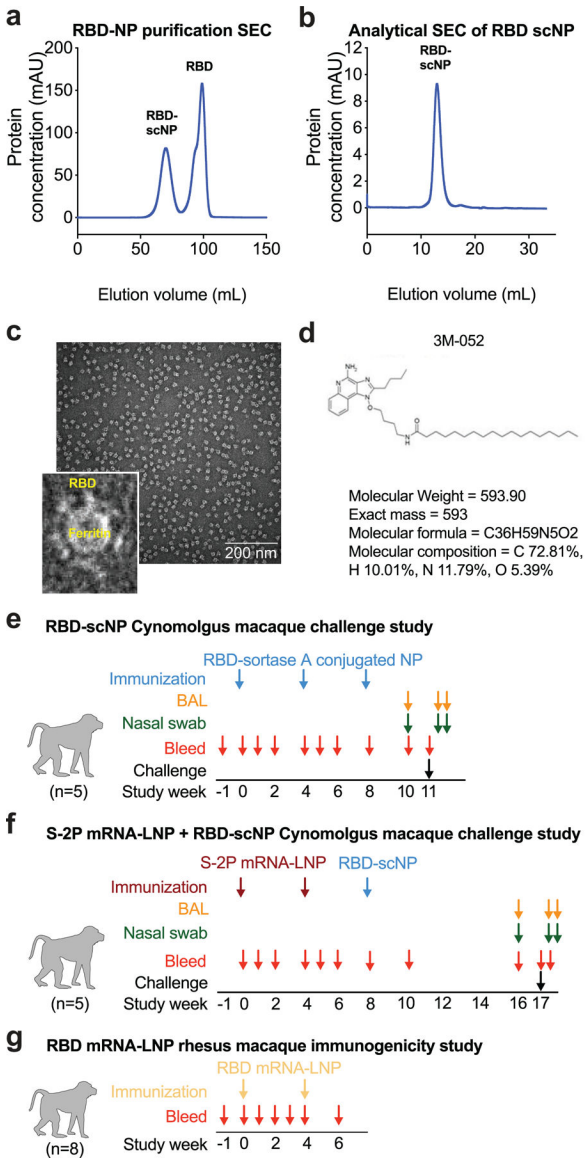

Extended Data Figure 1. Molecular and structural characterization of the SARS-CoV-2 RBD sortase A conjugated nanoparticle.

a Size exclusion chromatography of RBD and ferritin sortase conjugation. The first peak shows conjugated protein. The second peak contains unconjugated RBD.

b Analytical size exclusion trace shows a homogenous nanoparticle preparation.

c Negative stain electron microscopy image of RBD-scNPs on a carbon grid. Inset shows a zoomed image of RBD-scNP. The zoomed image shows RBD molecules arrayed around the outside of the ferritin nanoparticle. A representative image from the 31 images taken of the micrograph to visualize 13,827 total particles is shown.

d Chemical structure of toll-like receptor 7 and 8 agonist 3M-052. Alum formulation of 3M-052 was used to adjuvant RBD-scNP immunization.

e RBD-scNP immunization regimen used for vaccination of cynomolgus macaques (N=5). Blue arrows indicate timepoints for intramuscular immunizations with RBD-scNP (100 μg) adjuvanted with 3M-052 (5 μg 3M-052 plus 500 μg Alum). Bronchoalveolar lavage (BAL, orange arrows) and nasal swab (green arrows) fluids were collected 7 days before, 2 days after, and 4 days after intratracheal/intranasal SARS-CoV-2 challenge (black arrow).
f Transmembrane, diproline-stabilized spike (S-2P) mRNA-LNP prime, RBD-scNP boost vaccination of cynomolgus macaques (N=5). Maroon arrows indicate timepoints for S-2P mRNA-LNP immunization (50 μg mRNA dose). Blue arrows are the same as in **a**. Macaques were challenged 9 weeks after RBD-scNP boost (week 17 of the study). BAL and nasal swab fluids were collected as in **a**. Macaques were challenged at week 17 (black arrow).
g Monomeric RBD mRNA-LNP immunization of rhesus macaques (N=8). Tan arrows indicate timepoints for RBD mRNA-LNP immunization (50 μg mRNA dose). Blood was collected throughout each study as shown by red arrows in all panels.

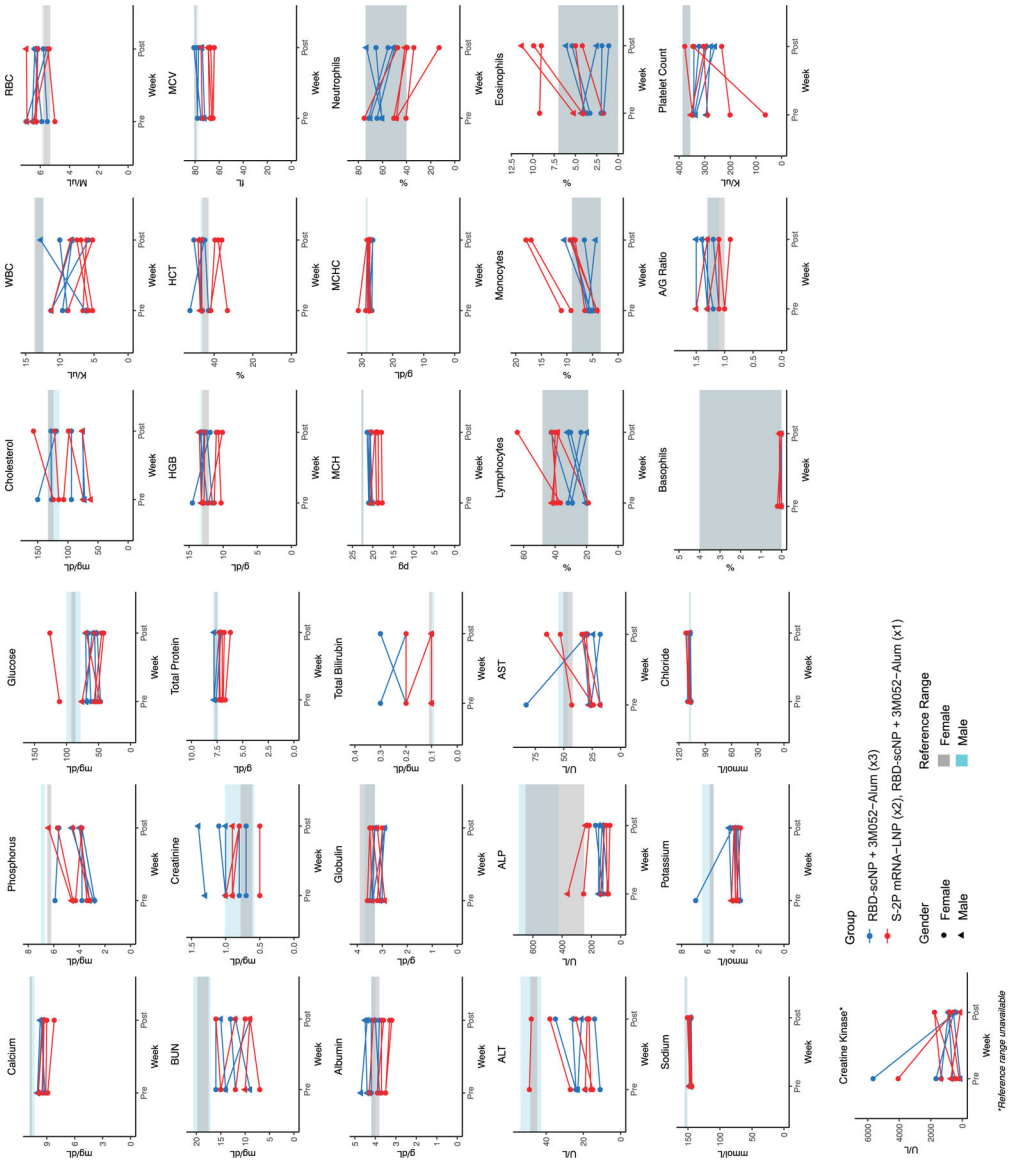

Extended Data Figure 2. Blood chemical analysis and blood cell counts in RBD-scNP and S-2P mRNA-LNP-vaccinated macaques.

Each graph shows values for individual macaques before vaccination and 4 weeks after the RBD-scNP (week 8) or 6 weeks after the second S-2P mRNA-LNP immunization (week 10). RBD-scNP-immunized macaques are shown as blue symbols, and S-2P mRNA-LNP immunized macaques are shown as red symbols. The reference range for each value is shown as gray shaded area for female macaques and cyan shaded area for male macaques. Creatine kinase does not have a reference range indicated. Males are shown as circles and females are shown as triangles.

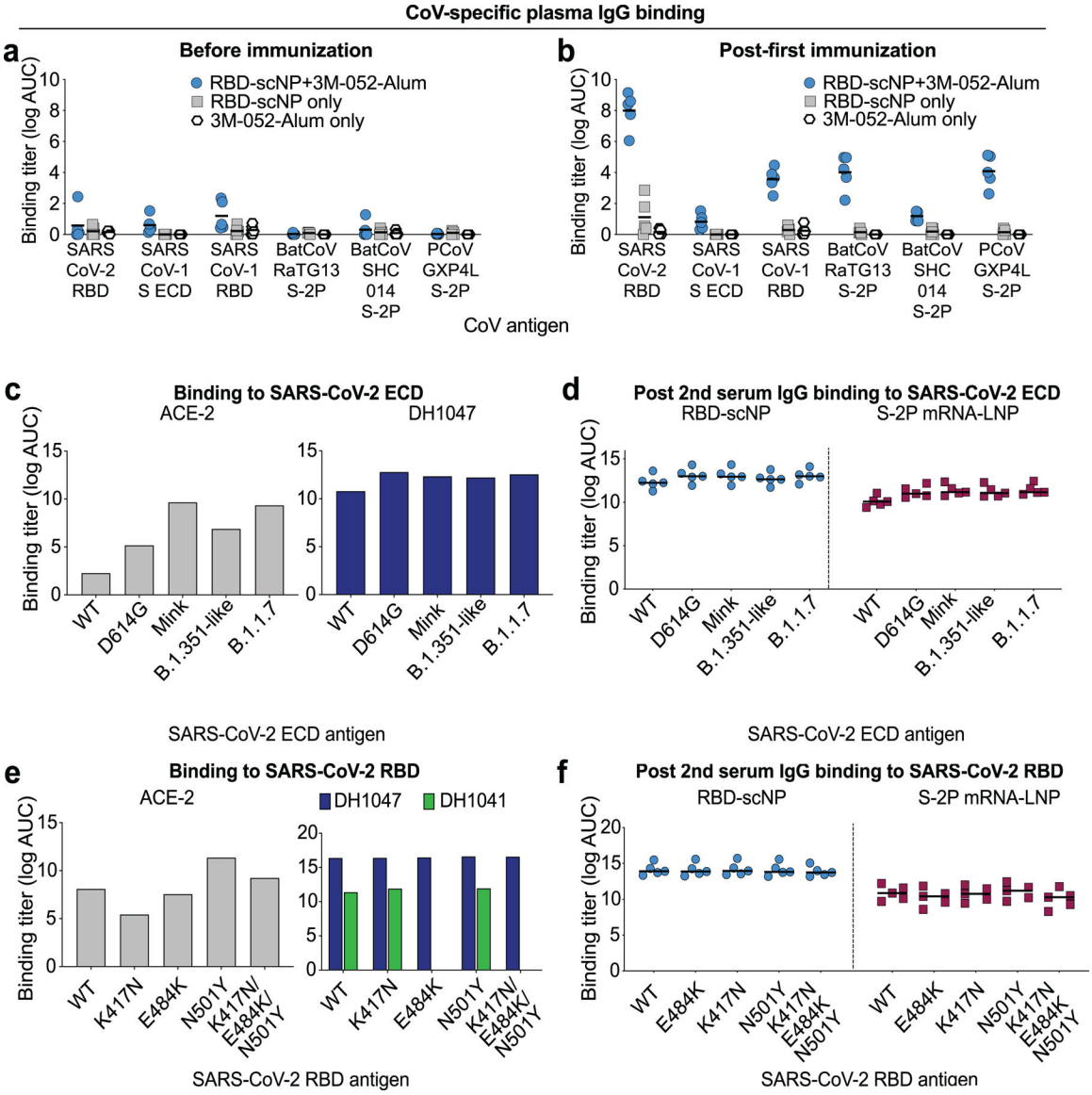

Extended Data Figure 3. ACE-2, RBD neutralizing antibody, and post-vaccination macaque plasma IgG binding to SARS-CoV-2 Spike variants.

a,b Plasma IgG from macaques prior to immunization or after being immunized once with RBD-scNP adjuvanted with 3M-052-Alum (blue), RBD-scNP only (gray), or 3M-052-Alum only (white). Binding titers as log AUC were determined **a** before or **b** two weeks after a single immunization. Horizontal bars are the group mean. ECD, ectodomain; S-2P, diproline-stabilized spike.

c ACE2 receptor and cross-nAbDH1047 ELISA binding to SARS-CoV-2 Spike ectodomain (ECD) based on a Danish mink (H69/V70deI/Y453F/D614G/I692V), B.1.351-like (K417N/E484K/N501Y/D614G), and B.1.1.7 (H69/V70del/Y144del/N501Y/A570D/D614G/P681H/T716I/S982A/D1118H) strains. Titers are shown as area under the log-transformed curve (log AUC).

d RBD-scNP and S-2P mRNA-LNP-immunized macaque serum IgG ELISA binding to SARS-CoV-2 Spike variants shown in **c**. Serum was tested after two immunizations. Horizontal bars are the group mean.

e ACE2 receptor (gray), cross-nAbDH1047 (navy), and ACE2 binding site-targeting neutralizing antibody DH1041 (green) ELISA binding to SARS-CoV-2 Spike RBD monomers. RBD variants contain a subset of mutations found in circulating B.1.351 and P.1 virus strains. Titers are shown as area under the log-transformed curve (log AUC).

f RBD-scNP and S-2P mRNA-LNP-immunized macaque serum IgG ELISA binding to SARS-CoV-2 Spike RBD variants shown in **e**. Serum was tested after two immunizations. Horizontal bars are the group mean.

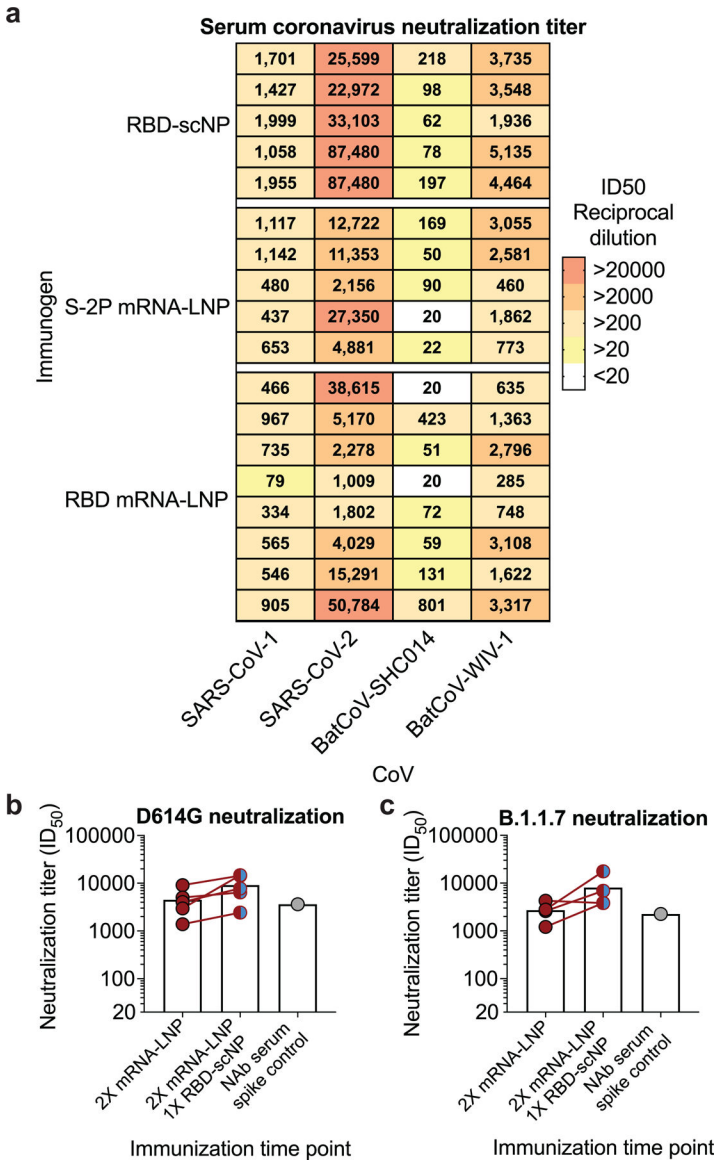

Extended Data Figure 4. Cross-neutralizing antibodies are elicited by recombinant protein RBD-scNP and mRNA-LNP immunization.

a Each row shows neutralization titer for an individual macaque immunized with one of the three immunogens. A reciprocal serum dilution titer of 87,480 is the upper limit of detection and 20 is the lower limit of detection for this assay. Titers are derived from a nonlinear regression curve fit to the average of duplicate measurements.

b,c Serum neutralization titers elicited by two S-2P mRNA-LNP immunizations were boosted by a subsequent RBD-scNP immunization. Serum neutralization of a SARS-CoV-2 D614G and b SARS-CoV-2 B.1.1.7 pseudovirus infection of ACE2-expressing 293 cells. Neutralization titers are ID50 as reciprocal serum dilution for serum collected two weeks after the second (week 6) and third immunization (week 10). Each symbol connected by a line represents the titer for an individual macaque before and after RBD-scNP immunization. Normal human serum spiked with DH1043 was used as a positive control.

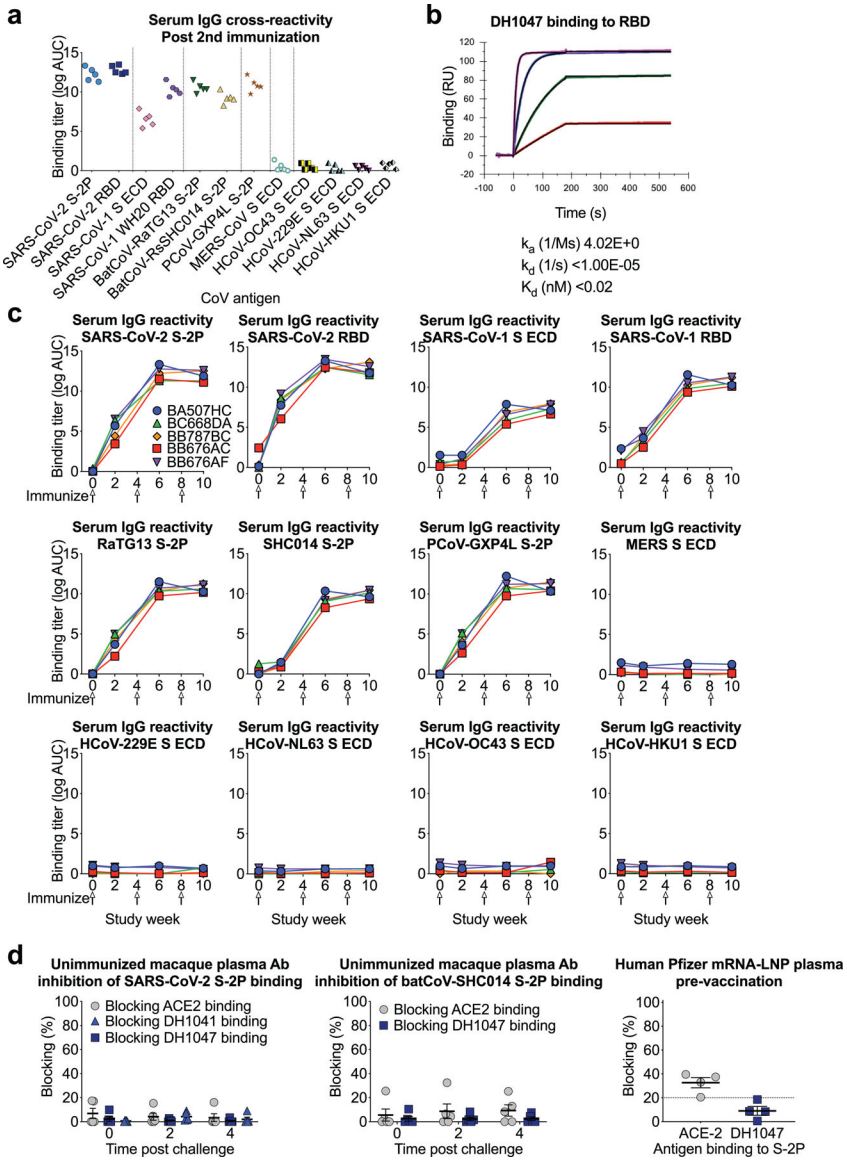

Extended Data Figure 5. Cross-reactive plasma antibody responses elicited by RBD-NP immunization in macaques.

a Plasma IgG from macaques immunized twice with RBD-scNP binds to Spike from human, bat, and pangolin SARS-related coronavirus Spike (S) in ELISA, but not endemic human coronaviruses or MERS-CoV. ECD, ectodomain.

b Determination of DH1047 antigen binding fragment (Fab) binding kinetics to RBD monomer by surface plasmon resonance. Each curve shows a different concentration of DH1047 Fab. Binding kinetics are shown to the right from a 1:1 model fit.

c Time course of vaccinated macaque plasma IgG binding to human, bat, and pangolin coronavirus S protein by ELISA. Each curve indicates the binding titer for an individual macaque. Arrows indicate immunization time points.

d Unimmunized macaque plasma antibody blocking of SARS-CoV-2 S-2P (left) and batCoV-SHC014 (middle) binding to ACE2-Fc, RBD neutralizing antibody DH1041, and RBD cross-nAbDH1047. (Right) Blocking activity in the serum of humans immunized with Pfizer S-2P mRNA-LNP vaccine (N=4). Each symbol represents an individual human or macaque. Bars indicate group mean±s.e.m.

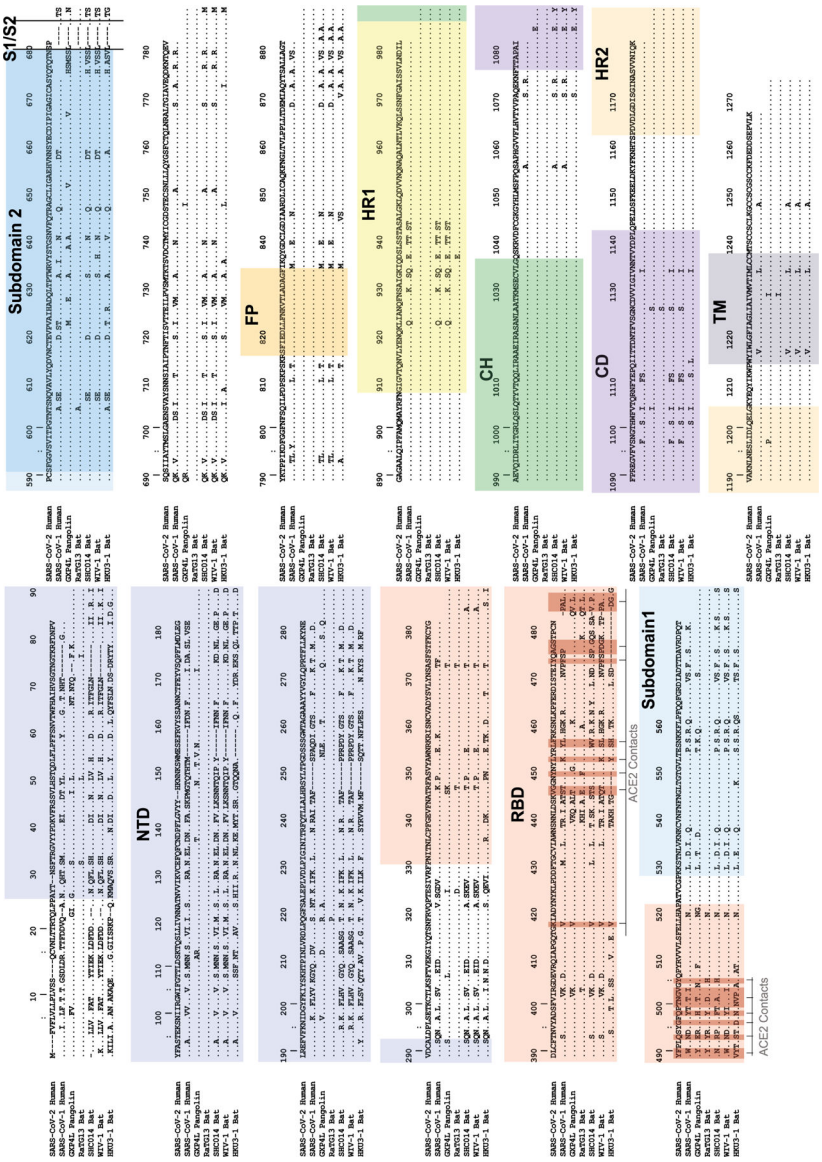

Extended Data Figure 6. Multiple Sequence Alignment of Spike Protein from a Representative Set of Group 2b Betacoronaviruses.

SARS-CoV-2 Wuhan-1 spike protein numbering is shown. NTD=N-terminal domain; RBD=receptor binding domain; S1/S2=SARS2 furin cleavage site; FP=fusion peptide; HR1=heptad repeat 1; HR2=heptad repeat 2; CH=central helix; CD=connecting domain; TM=transmembrane domain. ACE2 contact positions in SARS2 (calculated from PDB coordinates 6MOJ and 6LZG) are highlighted in dark red.

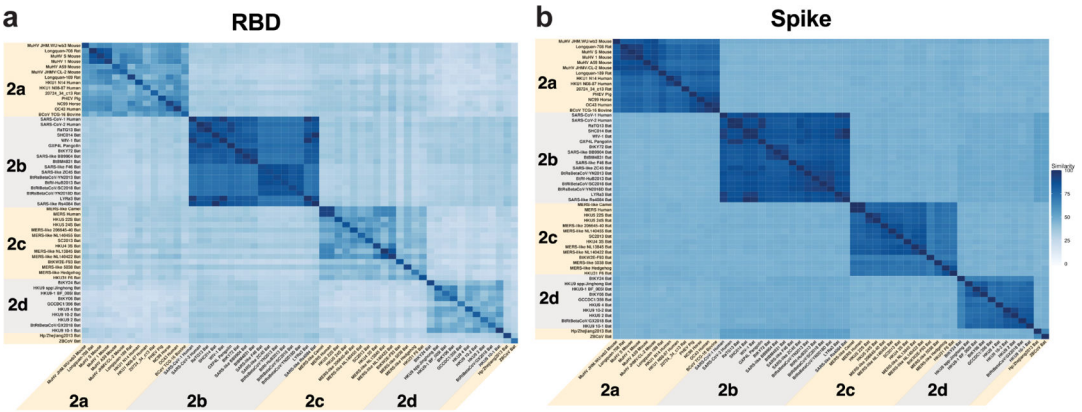

c

Group 2a
Longquan-708 Rat
MuHV S Mouse
MuHV 1 Mouse
MuHV A59 Mouse
MuHV JHMV/CL-2 Mouse
Longquan-189 Rat
HKU1 N14 Human
HKU1 N0S-87 Human
20724_34_C13 Rat
PHEV Pig
NC99 Horse
OC43 Human
BCoV TCG-16 Bovine

Group 2b
SARS-CoV-1 Human
SARS-CoV-2 Human
RaTG13 Bat
SHC014 Bat
WIV-1 Bat
GXP4L Pangolin
BtKY72 Bat
SARS-like BB9904 Bat
BtBM4831 Bat
SAAS-like F46 Bat
SAAS-like ZC45 Bat
BtRsBetaCoVIYN2013 Bat
BtRI-HuB2013 Bat
BtRIBetaCoV/SC2018 Bat
BtRsBetaCoV/YN2018D Bat
LVRa3 Bat
SARS-like As4084 Bat

Group 2c
MEAS-like Camel
MERS Human
HKU5 22S Bat
HKU5 24S Bat
MERS-like 206645-40 Bat
MEAS-like NL140455 Bat
SC2013 Bat
HKU4 3S Bat
MEAS-like NL13845 Bat
MEAS-like NL140422 Bat
BtKW2E-F93 Bat
MERS-like 5038 Bat
MEAS-like Hedgehog
HKU31 F6 Bat

Group 2d
BtKY24 Bat
HKU9 spp/JInghong Bat
HKU9-1 BF_0051 Bat
BtKY06 Bat
GCCDC1I356 Bat
HKU9 4 Bat
HKU9 10-2 Bat
HKU9 2 Bat
BtRtBetaCoV/GX2018 Bat
HKU910-1 Bat

Ungrouped
Hp/ZheJlang2013 Bat
ZBCoV Bat

d

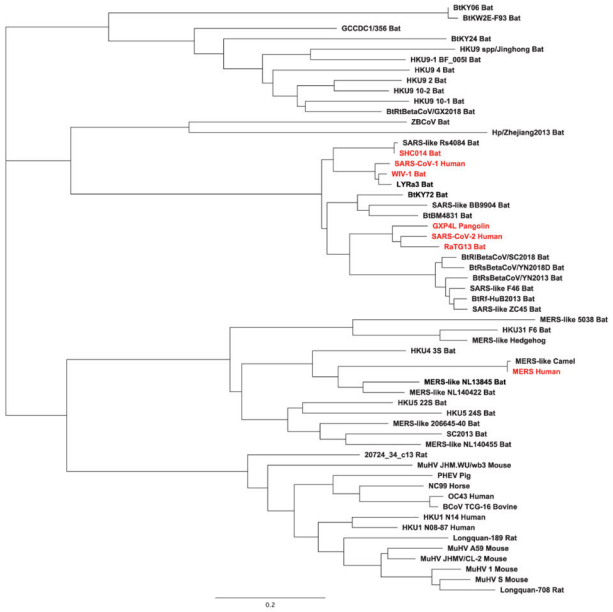

Extended Data Figure 7. Sequence conservation among SARS-related betaCoV, MERS-CoV, and endemic human CoVs.

a,b Sequence similarity of **a** RBD and **b** spike protein for representative betacoronaviruses. Heatmaps displaying pairwise amino acid sequence similarity for 57 representative betacoronaviruses. Dark blue shading indicates high sequence similarity.

c List of viruses used for alignments in **a** and Fig. 3f.

d Phylogenetic tree of representative betacoronavirus RBD sequences. Group 2b betaCoVs of interest are shown highlighted in red. Branch length units are substitutions per site.

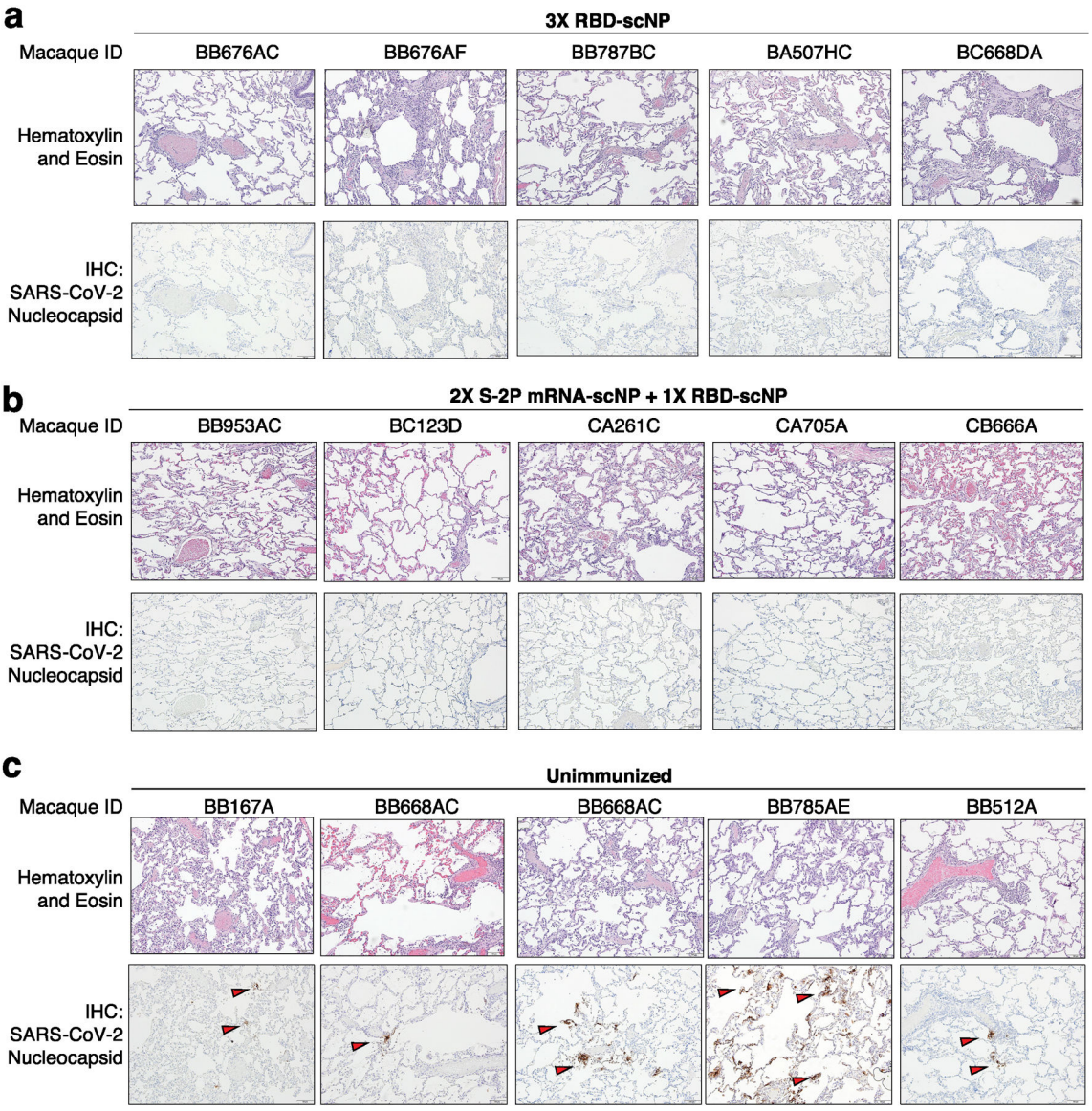

Extended Data Figure 8. Histology and immunohistochemistry of lung tissue collected seven days after SARS-CoV-2 WA-1 intratracheal and intranasal challenge.

a-c Macaques were immunized **a** thrice with RBD-scNP, **b** twice with S-2P mRNA-LNP and once with RBD-scNP, or **c** unimmunized. Each column shows results from an individual macaque. The macaque identification number is shown above each column. Hematoxylin and eosin stain of lung sections are shown on the top row, with nucleocapsid immunohistochemistry shown on the bottom row for each macaque. Red arrows indicate site of antigen positivity. All images are shown at 10X magnification with 100 micron scale bars shown in the bottom right corner.

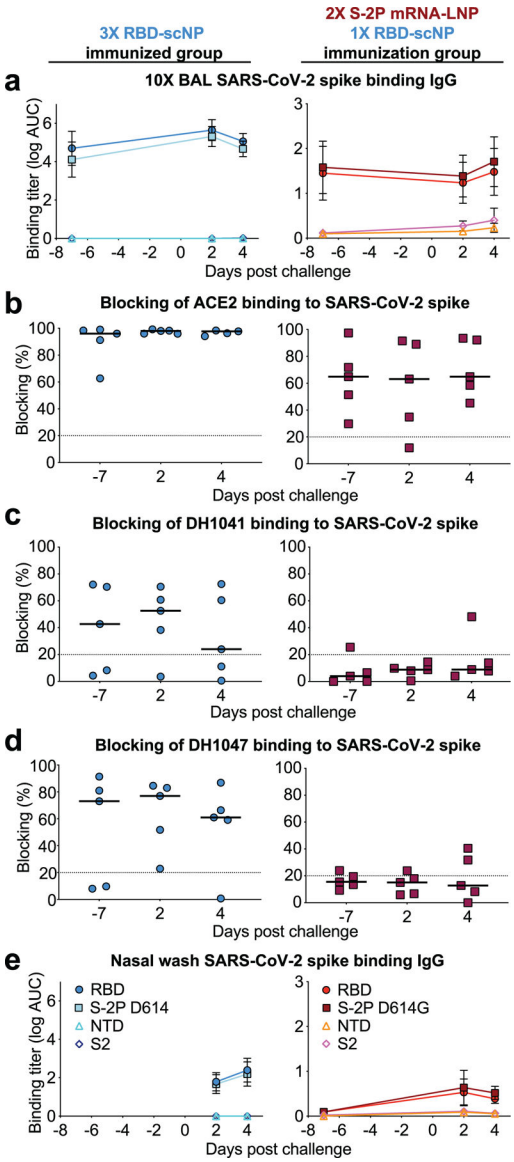

Extended Data Figure 9. Mucosal SARS-CoV-2 IgG responses in bronchoalveolar lavage (BAL) and nasal wash fluids before and after SARS-CoV-2 challenge.

a ELISA binding titers for SARS-CoV-2-specific IgG in 10X BAL fluid from macaques immunized with (blue symbols, left column) RBD-scNP three times or S-2P mRNA-LNP twice and RBD-scNP once (red symbols, left column). Day -7 BAL fluid was collected at week 10 or 16 for the RBD-scNP alone group or the S-2P mRNA-LNP/RBD-scNP group respectively. Group mean±s.e.m. are shown (N=5).

b-d 10X BAL fluid blocking of ACE2, RBD neutralizing antibody DH1041, and cross-nAbDH1047 binding to SARS-CoV-2 D614G stabilized spike ectodomain. A black horizontal bar indicates the group mean blocking percentage. Blocking above 20% (above the dashed line) is considered positive.

e Neat nasal wash fluid from RBD-scNP-immunized or S-2P mRNA-LNP/RBD-scNP-immunized macaques. Day -7 nasal wash fluid was collected at week 16 and 2 and 4 days post challenge for the S-2P mRNA-LNP/RBD-scNP group. Nasal wash fluid was

unavailable for the RBD-scNP before challenge, but was collected 2 and 4 days after the week 11 challenge. Group mean±s.e.m. are shown (N=5).

Extended Data Table 1.

Scoring of Hematoxylin and eosin (H&E) staining and immunohistochemistry (IHC) of macaque lung tissue collected seven days after challenge.

Group	Macaque ID	Tissue	H&E (Lc; Rm; Rc)	SARS-Cov-2 N IHC (Lc; Rm; Rc)
3X RBD-scNP	BB676AC	lung	+/−; +; +	−; −; −
	BB676AF	lung	++; ++; +	−; −; −
	BB787BC	lung	++; +; +	−; −; −
	BA507HC	lung	+, +, +/−	−; −; −
	BC668DA	lung	+/−, ++, ++	−; −; −
2X S-2P mRNA-LNP + 1X RBD-scNP	BB953AC	lung	+/−; +/−; +/−	−; −; −
	BC123D	lung	+/−; −; +/−	−; −; −
	CA261C	lung	+/−; +; +	−; −; −
	CA705A	lung	+/−; −; −	−; −; −
	CB666A	lung	+/−; +; +	−; −; −
Unimmunized	20201C	lung	+; +; +	+/−; −; −
	BB167A	lung	++; ++; ++	+/−; −; −
	BB668AC	lung	++; +; +	+/−; ++; ++
	BB785AE	lung	+/−; +++; +	−; ++; ++
	BB512A	lung	+; ++; ++	+; +/−; +

[a] H&E (inflammation): − = minimal – absent, +/− = minimal – mild, + = mild to moderate, ++ = moderate-severe, +++ = severe.

[b] IHC (SARS-CoV-2 nucleocapsid Ag positive foci): − = no SARS-CoV-2 Ag detected, +/− = rare- occasional, + = occasional-multiple), ++ = multiple- numerous (foci often larger), +++ = numerous.

Supplementary Material

Refer to Web version on PubMed Central for supplementary material.

ACKNOWLEDGEMENTS

We thank Victoria Gee-Lai, Margaret Deyton, Charlene McDanal, Brian Watts, and Kenneth Cronin for technical assistance. We thank Elizabeth Donahue for program management and assistance with manuscript preparation. We thank P.J.C. Lin and Y.K. Tam from Acuitas Therapeutics for providing lipid nanoparticles. We thank John Harrison, Alex Granados, Adrienne Goode, Anthony Cook, Alan Dodson, Katelyn Steingrebe, Bridget Bart, Laurent Pessaint, Alex VanRy, Daniel Valentin, Amanda Strasbaugh, and Mehtap Cabus for assistance with macaque studies. We thank Shelby O'Connor and John James Baczenas at the Dept. of Pathology & Laboratory Medicine, University of Wisconsin-Madison for sequencing support. The following reagent was deposited by the Centers for Disease Control and Prevention and obtained through BEI Resources, NIAID, NIH: SARS-Related Coronavirus 2, Isolate USA-WA1/2020, NR-52281. Supported by a grant from the State of North Carolina with funds from the federal CARES Act, by funds from NIH, NIAID, DAIDS grant AI142596 (BFH), and by R01AI157155 (RSB) and U54 CA260543 (RSB). This project was also supported by the North Carolina Policy Collaboratory at the University of North Carolina at Chapel Hill with funding from the North Carolina Coronavirus Relief Fund established and appropriated by the North Carolina General Assembly. This study was also supported by funding from an NIH F32 AI152296, a Burroughs Wellcome Fund Postdoctoral Enrichment Program Award, and was previously supported by an NIH NIAID T32 AI007151 (all three awarded to DRM). COVID sample processing was performed in the Duke Regional Biocontainment Laboratory, which received partial support for

construction from the NIH/NIAD (UC6AI058607; GDS) with support from a cooperative agreement with DOD/DARPA (HR0011–17-2–0069; GDS).

REFERENCES

1. Wang C, Horby PW, Hayden FG & Gao GF A novel coronavirus outbreak of global health concern. Lancet 395, 470–473, doi:10.1016/s0140-6736(20)30185-9 (2020). [PubMed: 31986257]
2. Zaki AM, van Boheemen S, Bestebroer TM, Osterhaus AD & Fouchier RA Isolation of a novel coronavirus from a man with pneumonia in Saudi Arabia. N Engl J Med 367, 1814–1820, doi:10.1056/NEJMoa1211721 (2012). [PubMed: 23075143]
3. Zhong NS et al. Epidemiology and cause of severe acute respiratory syndrome (SARS) in Guangdong, People's Republic of China, in February, 2003. Lancet 362, 1353–1358, doi:10.1016/s0140-6736(03)14630-2 (2003). [PubMed: 14585636]
4. Zhu N et al. A Novel Coronavirus from Patients with Pneumonia in China, 2019. N Engl J Med 382, 727–733, doi:10.1056/NEJMoa2001017 (2020). [PubMed: 31978945]
5. Zhou P et al. A pneumonia outbreak associated with a new coronavirus of probable bat origin. Nature 579, 270–273, doi:10.1038/s41586-020-2012-7 (2020). [PubMed: 32015507]
6. Li W et al. Bats are natural reservoirs of SARS-like coronaviruses. Science 310, 676–679, doi:10.1126/science.1118391 (2005). [PubMed: 16195424]
7. Olival KJ et al. Host and viral traits predict zoonotic spillover from mammals. Nature 546, 646–650, doi:10.1038/nature22975 (2017). [PubMed: 28636590]
8. Sabir JS et al. Co-circulation of three camel coronavirus species and recombination of MERS-CoVs in Saudi Arabia. Science 351, 81–84, doi:10.1126/science.aac8608 (2016). [PubMed: 26678874]
9. Ge XY et al. Isolation and characterization of a bat SARS-like coronavirus that uses the ACE2 receptor. Nature 503, 535–538, doi:10.1038/nature12711 (2013). [PubMed: 24172901]
10. Guan Y et al. Isolation and characterization of viruses related to the SARS coronavirus from animals in southern China. Science 302, 276–278, doi:10.1126/science.1087139 (2003). [PubMed: 12958366]
11. Xiao K et al. Isolation of SARS-CoV-2-related coronavirus from Malayan pangolins. Nature 583, 286–289, doi:10.1038/s41586-020-2313-x (2020). [PubMed: 32380510]
12. Menachery VD, Graham RL & Baric RS Jumping species-a mechanism for coronavirus persistence and survival. Curr Opin Virol 23, 1–7, doi:10.1016/j.coviro.2017.01.002 (2017). [PubMed: 28214731]
13. Pinto D et al. Cross-neutralization of SARS-CoV-2 by a human monoclonal SARS-CoV antibody. Nature 583, 290–295, doi:10.1038/s41586-020-2349-y (2020). [PubMed: 32422645]
14. Wec AZ et al. Broad neutralization of SARS-related viruses by human monoclonal antibodies. Science 369, 731–736, doi:10.1126/science.abc7424 (2020). [PubMed: 32540900]
15. Li D et al. The functions of SARS-CoV-2 neutralizing and infection-enhancing antibodies in vitro and in mice and nonhuman primates. bioRxiv, doi:10.1101/2020.12.31.424729 (2021).
16. Shi R et al. A human neutralizing antibody targets the receptor-binding site of SARS-CoV-2. Nature 584, 120–124, doi:10.1038/s41586-020-2381-y (2020). [PubMed: 32454512]
17. Ju B et al. Human neutralizing antibodies elicited by SARS-CoV-2 infection. Nature 584, 115–119, doi:10.1038/s41586-020-2380-z (2020). [PubMed: 32454513]
18. Robbiani DF et al. Convergent antibody responses to SARS-CoV-2 in convalescent individuals. Nature 584, 437–442, doi:10.1038/s41586-020-2456-9 (2020). [PubMed: 32555388]
19. Zost SJ et al. Potently neutralizing and protective human antibodies against SARS-CoV-2. Nature 584, 443–449, doi:10.1038/s41586-020-2548-6 (2020). [PubMed: 32668443]
20. Liu L et al. Potent neutralizing antibodies against multiple epitopes on SARS-CoV-2 spike. Nature 584, 450–456, doi:10.1038/s41586-020-2571-7 (2020). [PubMed: 32698192]
21. Hansen J et al. Studies in humanized mice and convalescent humans yield a SARS-CoV-2 antibody cocktail. Science 369, 1010–1014, doi:10.1126/science.abd0827 (2020). [PubMed: 32540901]
22. Brouwer PJM et al. Potent neutralizing antibodies from COVID-19 patients define multiple targets of vulnerability. Science 369, 643–650, doi:10.1126/science.abc5902 (2020). [PubMed: 32540902]

23. Rogers TF et al. Isolation of potent SARS-CoV-2 neutralizing antibodies and protection from disease in a small animal model. Science 369, 956–963, doi:10.1126/science.abc7520 (2020). [PubMed: 32540903]
24. Piccoli L et al. Mapping Neutralizing and Immunodominant Sites on the SARS-CoV-2 Spike Receptor-Binding Domain by Structure-Guided High-Resolution Serology. Cell 183, 1024–1042.e1021, doi:10.1016/j.cell.2020.09.037 (2020). [PubMed: 32991844]
25. Burton DR & Walker LM Rational Vaccine Design in the Time of COVID-19. Cell Host Microbe 27, 695–698, doi:10.1016/j.chom.2020.04.022 (2020). [PubMed: 32407707]
26. Cohen AA et al. Mosaic nanoparticles elicit cross-reactive immune responses to zoonotic coronaviruses in mice. Science, doi:10.1126/science.abf6840 (2021).
27. Ma X et al. Nanoparticle Vaccines Based on the Receptor Binding Domain (RBD) and Heptad Repeat (HR) of SARS-CoV-2 Elicit Robust Protective Immune Responses. Immunity 53, 1315–1330 e1319, doi:10.1016/j.immuni.2020.11.015 (2020). [PubMed: 33275896]
28. Bangaru S et al. Structural analysis of full-length SARS-CoV-2 spike protein from an advanced vaccine candidate. Science 370, 1089–1094, doi:10.1126/science.abe1502 (2020). [PubMed: 33082295]
29. Walls AC et al. Elicitation of Potent Neutralizing Antibody Responses by Designed Protein Nanoparticle Vaccines for SARS-CoV-2. Cell 183, 1367–1382 e1317, doi:10.1016/j.cell.2020.10.043 (2020). [PubMed: 33160446]
30. Saunders KO et al. Targeted selection of HIV-specific antibody mutations by engineering B cell maturation. Science 366, doi:10.1126/science.aay7199 (2019).
31. Fox CB et al. Adsorption of a synthetic TLR7/8 ligand to aluminum oxyhydroxide for enhanced vaccine adjuvant activity: A formulation approach. J Control Release 244, 98–107, doi:10.1016/j.jconrel.2016.11.011 (2016). [PubMed: 27847326]
32. Korber B et al. Tracking Changes in SARS-CoV-2 Spike: Evidence that D614G Increases Infectivity of the COVID-19 Virus. Cell 182, 812–827.e819, doi:10.1016/j.cell.2020.06.043 (2020). [PubMed: 32697968]
33. Baden LR et al. Efficacy and Safety of the mRNA-1273 SARS-CoV-2 Vaccine. N Engl J Med, doi:10.1056/NEJMoa2035389 (2020).
34. Polack FP et al. Safety and Efficacy of the BNT162b2 mRNA Covid-19 Vaccine. N Engl J Med 383, 2603–2615, doi:10.1056/NEJMoa2034577 (2020). [PubMed: 33301246]
35. Galloway SE et al. Emergence of SARS-CoV-2 B.1.1.7 Lineage - United States, December 29, 2020-January 12, 2021. MMWR Morb Mortal Wkly Rep 70, 95–99, doi:10.15585/mmwr.mm7003e2 (2021). [PubMed: 33476315]
36. Leung K, Shum MH, Leung GM, Lam TT & Wu JT Early transmissibility assessment of the N501Y mutant strains of SARS-CoV-2 in the United Kingdom, October to November 2020. Euro Surveill 26, doi:10.2807/1560-7917.ES.2020.26.1.2002106 (2021).
37. Faria NR et al. Genomic characterisation of an emergent SARS-CoV-2 lineage in Manaus: preliminary findings. Virological (2021).
38. Tegally H et al. Sixteen novel lineages of SARS-CoV-2 in South Africa. Nat Med, doi:10.1038/s41591-021-01255-3 (2021).
39. Wibmer CK et al. SARS-CoV-2 501Y.V2 escapes neutralization by South African COVID-19 donor plasma. bioRxiv, doi:10.1101/2021.01.18.427166 (2021).
40. Lassaunière R et al. SARS-CoV-2 spike mutations arising in Danish mink and their spread to humans, <https://files.ssi.dk/Mink-cluster-5-short-report_AFO2> (2021).
41. Menachery VD et al. A SARS-like cluster of circulating bat coronaviruses shows potential for human emergence. Nat Med 21, 1508–1513, doi:10.1038/nm.3985 (2015). [PubMed: 26552008]
42. Menachery VD et al. SARS-like WIV1-CoV poised for human emergence. Proc Natl Acad Sci U S A 113, 3048–3053, doi:10.1073/pnas.1517719113 (2016). [PubMed: 26976607]
43. Liu H et al. Cross-Neutralization of a SARS-CoV-2 Antibody to a Functionally Conserved Site Is Mediated by Avidity. Immunity 53, 1272–1280 e1275, doi:10.1016/j.immuni.2020.10.023 (2020). [PubMed: 33242394]
44. Muik A et al. Neutralization of SARS-CoV-2 lineage B.1.1.7 pseudovirus by BNT162b2 vaccine-elicited human sera. Science, doi:10.1126/science.abg6105 (2021).

45. Wu K et al. mRNA-1273 vaccine induces neutralizing antibodies against spike mutants from global SARS-CoV-2 variants. bioRxiv, doi:10.1101/2021.01.25.427948 (2021).
46. Cele S et al. Escape of SARS-CoV-2 501Y.V2 variants from neutralization by convalescent plasma. medRxiv, 2021.2001.2026.21250224, doi:10.1101/2021.01.26.21250224 (2021).
47. Collier D et al. Impact of SARS-CoV-2 B.1.1.7 Spike variant on neutralisation potency of sera from individuals vaccinated with Pfizer vaccine BNT162b2. medRxiv, 2021.2001.2019.21249840, doi:10.1101/2021.01.19.21249840 (2021).
48. Wang Z et al. mRNA vaccine-elicited antibodies to SARS-CoV-2 and circulating variants. bioRxiv, 2021.2001.2015.426911, doi:10.1101/2021.01.15.426911 (2021).
49. Wibmer CK et al. SARS-CoV-2 501Y.V2 escapes neutralization by South African COVID-19 donor plasma. bioRxiv, 2021.2001.2018.427166, doi:10.1101/2021.01.18.427166 (2021).
50. Yu J et al. DNA vaccine protection against SARS-CoV-2 in rhesus macaques. Science 369, 806–811, doi:10.1126/science.abc6284 (2020). [PubMed: 32434945]
51. Mercado NB et al. Single-shot Ad26 vaccine protects against SARS-CoV-2 in rhesus macaques. Nature 586, 583–588, doi:10.1038/s41586-020-2607-z (2020). [PubMed: 32731257]

METHODS REFERENCES

52. Laczko D et al. A Single Immunization with Nucleoside-Modified mRNA Vaccines Elicits Strong Cellular and Humoral Immune Responses against SARS-CoV-2 in Mice. Immunity 53, 724–732 e727, doi:10.1016/j.immuni.2020.07.019 (2020). [PubMed: 32783919]
53. Pardi N et al. Zika virus protection by a single low-dose nucleoside-modified mRNA vaccination. Nature 543, 248–251, doi:10.1038/nature21428 (2017). [PubMed: 28151488]
54. Wrapp D et al. Cryo-EM structure of the 2019-nCoV spike in the prefusion conformation. Science 367, 1260–1263, doi:10.1126/science.abb2507 (2020). [PubMed: 32075877]
55. Hsieh CL et al. Structure-based Design of Prefusion-stabilized SARS-CoV-2 Spikes. bioRxiv, doi:10.1101/2020.05.30.125484 (2020).
56. Zhou T et al. Structure-Based Design with Tag-Based Purification and In-Process Biotinylation Enable Streamlined Development of SARS-CoV-2 Spike Molecular Probes. Cell Rep 33, 108322, doi:10.1016/j.celrep.2020.108322 (2020). [PubMed: 33091382]
57. Berry JD et al. Development and characterisation of neutralising monoclonal antibody to the SARS-coronavirus. J Virol Methods 120, 87–96, doi:10.1016/j.jviromet.2004.04.009 (2004). [PubMed: 15234813]
58. Coleman CM & Frieman MB Growth and Quantification of MERS-CoV Infection. Curr Protoc Microbiol 37, 15E 12 11–19, doi:10.1002/9780471729259.mc15e02s37 (2015).
59. Kint J, Maier HJ & Jagt E Quantification of infectious bronchitis coronavirus by titration in vitro and in ovo. Methods Mol Biol 1282, 89–98, doi:10.1007/978-1-4939-2438-7_9 (2015). [PubMed: 25720474]
60. Naldini L, Blömer U, Gage FH, Trono D & Verma IM Efficient transfer, integration, and sustained long-term expression of the transgene in adult rat brains injected with a lentiviral vector. Proc Natl Acad Sci U S A 93, 11382–11388, doi:10.1073/pnas.93.21.11382 (1996). [PubMed: 8876144]
61. Yount B et al. Reverse genetics with a full-length infectious cDNA of severe acute respiratory syndrome coronavirus. Proc Natl Acad Sci U S A 100, 12995–13000, doi:10.1073/pnas.1735582100 (2003). [PubMed: 14569023]
62. Scobey T et al. Reverse genetics with a full-length infectious cDNA of the Middle East respiratory syndrome coronavirus. Proc Natl Acad Sci U S A 110, 16157–16162, doi:10.1073/pnas.1311542110 (2013). [PubMed: 24043791]
63. Hou YJ et al. SARS-CoV-2 Reverse Genetics Reveals a Variable Infection Gradient in the Respiratory Tract. Cell 182, 429–446 e414, doi:10.1016/j.cell.2020.05.042 (2020). [PubMed: 32526206]
64. Edgar RC Search and clustering orders of magnitude faster than BLAST. Bioinformatics 26, 2460–2461, doi:10.1093/bioinformatics/btq461 (2010). [PubMed: 20709691]

65. Nakamura T, Yamada KD, Tomii K & Katoh K Parallelization of MAFFT for large-scale multiple sequence alignments. Bioinformatics 34, 2490–2492, doi:10.1093/bioinformatics/bty121 (2018). [PubMed: 29506019]

66. Valdar WS Scoring residue conservation. Proteins 48, 227–241, doi:10.1002/prot.10146 (2002). [PubMed: 12112692]

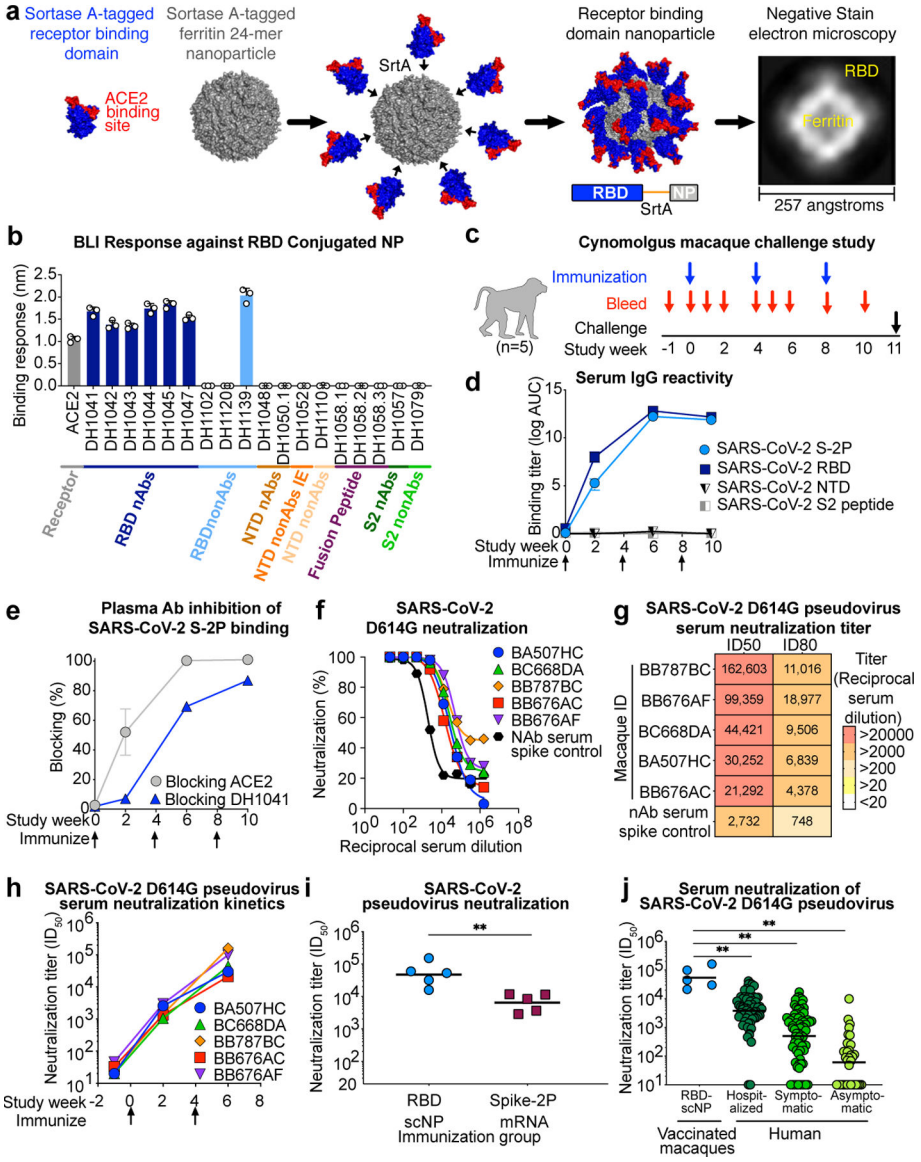

Figure 1. SARS-CoV-2 receptor binding domain (RBD) sortase-conjugated nanoparticles (scNPs) elicits extremely high titers of SARS-CoV-2 pseudovirus neutralizing antibodies (nAbs).

a SARS-CoV-2 RBD (blue and red) *Helicobacter pylori* ferritin (gray) nanoparticle sortase conjugation. A model and two-dimensional class average of negative stain electron microscopy of the resultant RBD nanoparticle are shown.

b Biolayer interferometry SARS-CoV-2 antibody and ACE2 receptor binding to RBD nanoparticles. N-terminal domain (NTD), infection enhancing non-neutralizing antibody (nonAbs IE), non-neutralizing antibody (nonAb). Symbols represent values from 3 independent experiments and bars represent the mean and standard error of the mean (s.e.m.).

c Cynomolgus macaque immunogenicity and challenge study design.

d Macaque serum IgG binding titer as area-under-the curve of the $\log_{10}$-transformed curve (log AUC) to recombinant SARS-CoV-2 stabilized Spike ectodomain (S-2P), RBD, NTD, and Fusion peptide (FP). Group mean±s.e.m. are shown in **d** and **e** (n = 5 macaques).

e Plasma antibody blocking of SARS-CoV-2 S-2P binding to ACE2-Fc and RBD neutralizing antibody DH1041.

f,g f Dose-dependent serum neutralization of SARS-CoV-2 D614G pseudovirus infection of ACE2-expressing 293T cells and **g** neutralization ID50 and ID80 titers. Serum was examined after two immunizations. The mean value of duplicates is shown in **f**.

h SARS-CoV-2 D614G pseudovirus serum neutralization titer over time for individual macaques.

i Serum neutralization ID50 titers from macaques immunized twice with protein RBD nanoparticles (blue) or nucleoside-modified mRNA-LNP expressing S-2P (burgundy) (** P = 0.0079, Two-tailed Exact Wilcoxon test, n = 5 macaques).

j Serum neutralization titers for macaques immunized twice with RBD-scNP (blue, n =5 macaques) or humans with asymptomatic infection (n=34 individuals), symptomatic infection (n=71 individuals), or hospitalized (n=60 individuals) (** P<0.01, Two-tailed Wilcoxon test). Horizontal bars are the group geometric mean in **i** and **j**. Pre-vaccination serum or nAb spiked serum were used as controls in **f**, **g,** and **h**.

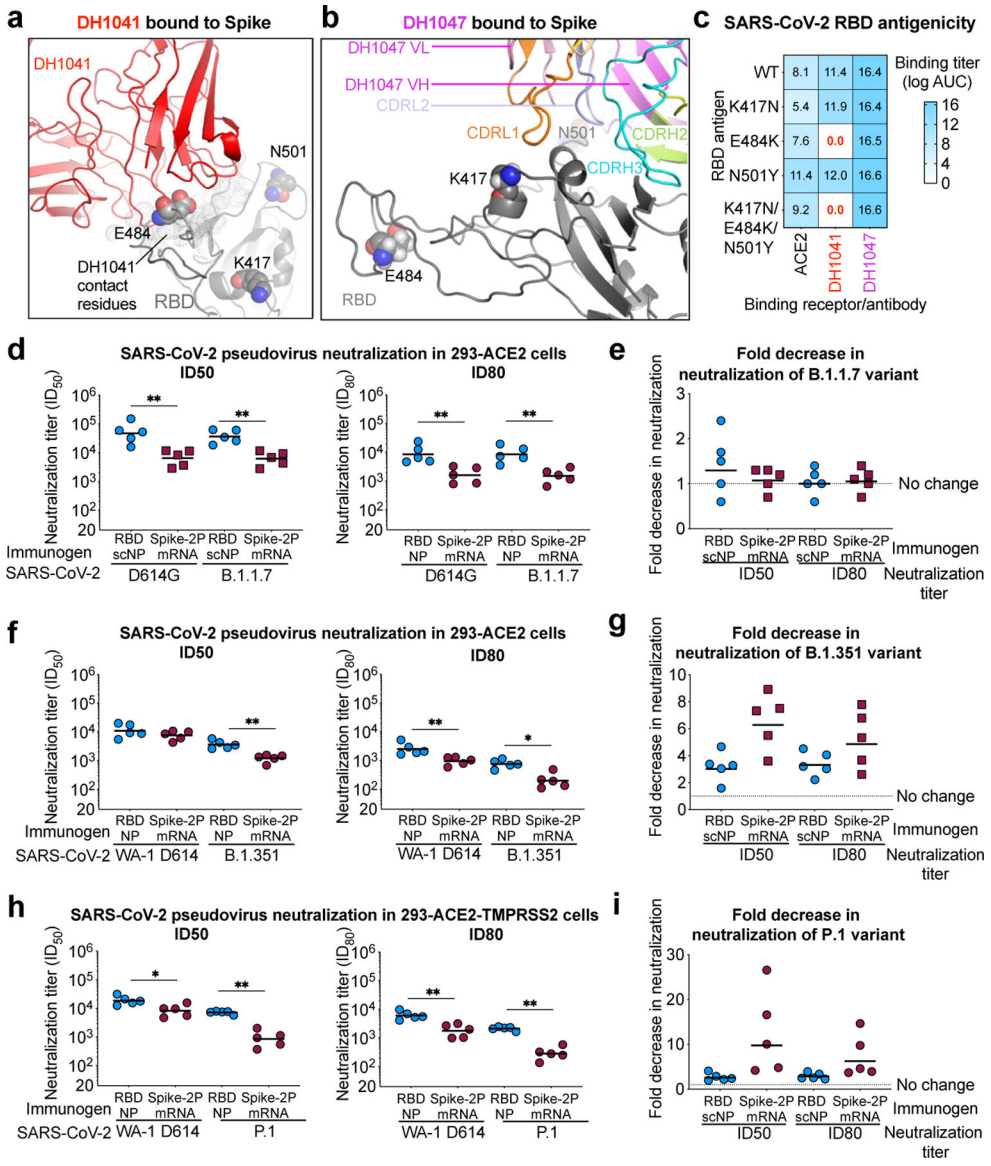

Figure 2. RBD-scNP immunization elicits higher titers of nAbs against more transmissible or neutralization-resistant SARS-CoV-2 variants than stabilized spike mRNA-LNP vaccination.

a,b The location of K417, E484, and N501 (spheres) present in the B.1.351 variant are shown in the cryo-EM structures of RBD nAbs **a** DH1041 (red) and **b** DH1047 (magenta) bound to the RBD (gray) of S trimers (PDB: 7LAA and 7LD1)[15].

c ACE2 receptor, DH1041, and DH1047 ELISA binding titer as log AUC for wildtype and mutant SARS-CoV-2 Spike RBD monomers.

d Serum neutralization ID50 (left) and ID80 titers for SARS-CoV-2 D614G and SARS-CoV-2 B.1.1.7 pseudoviruses from immunized macaques. Symbols represent individual macaques and horizontal bars are group means (**P = 0.0079, Two-tailed Exact Wilcoxon test, n = 5 macaques).

e Fold decrease in neutralization potency between neutralization of SARS-CoV-2 D614G and SARS-CoV-2 B.1.1.7 pseudoviruses. Fold change is shown for RBD-scNP-immunized

and mRNA-LNP-immunized macaques based ID50 (left) and ID80 (right) titers. Horizontal bars are the group mean.

f Vaccinated macaque serum neutralization ID50 (left) and ID80 titers (right) against WA-1 and B.1.351 pseudovirus. Symbols and horizontal bars are shown the same as in **d** (*P = 0.0159 and **P = 0.0079, Two-tailed Exact Wilcoxon test, n = 5 macaques).

g Fold decrease in neutralization potency between neutralization of SARS-CoV-2 WA-1 and B.1.351 pseudoviruses. Fold change is shown the same as in **e** .

h Vaccine-induced neutralization of SARS-CoV-2 WA-1 and P.1 pseudovirus infection of ACE2 and TMPRSS2-expressing 293 cells. Symbols and horizontal bars are shown the same as in **d** (*P = 0.0159 and **P = 0.0079, Two-tailed Exact Wilcoxon test, n = 5 macaques).

i Fold decrease in neutralization potency as shown in **e** between neutralization of SARS-CoV-2 WA-1 and P.1 pseudoviruses.

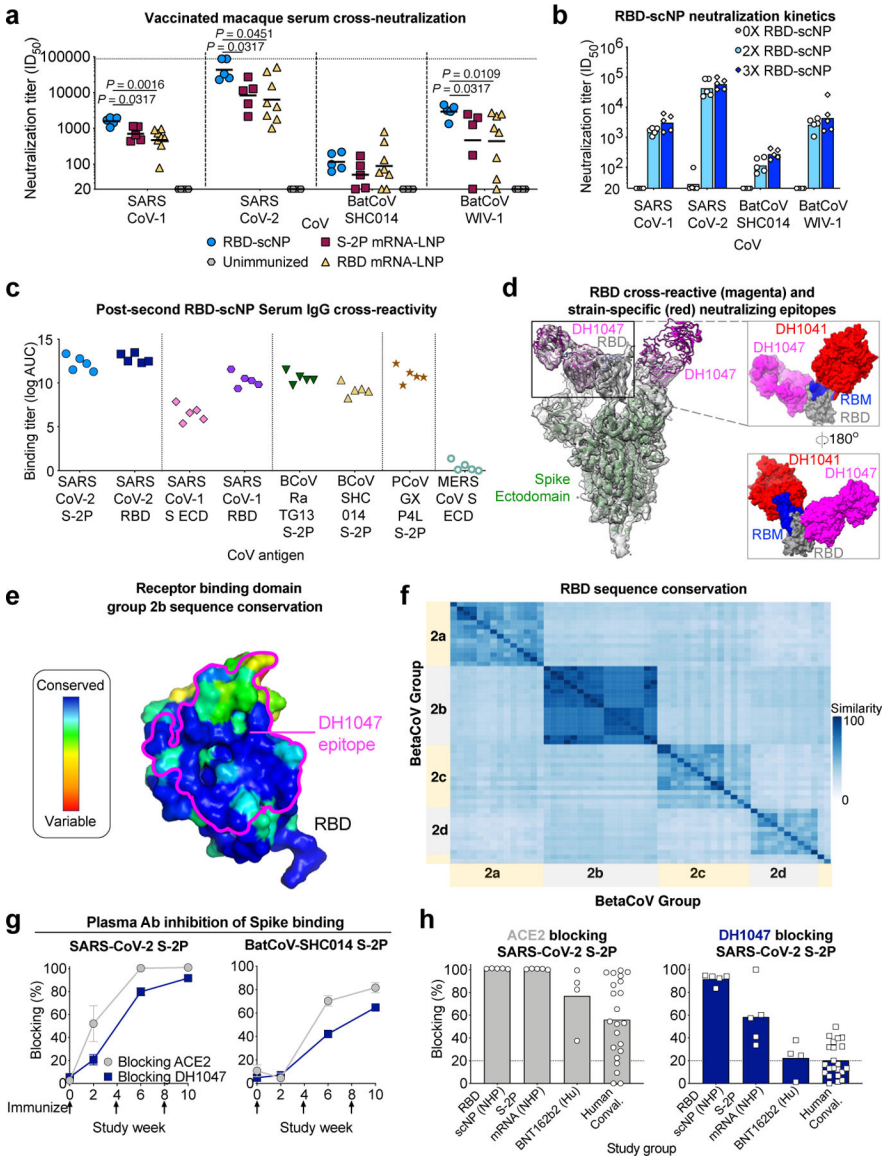

Figure 3. RBD-scNP vaccine induction of serum cross-neutralization of SARS-related betacoronavirus infection.

a Serum neutralization ID50 titers from macaques immunized twice with RBD-scNP, S-2P mRNA-LNP, or RBD mRNA-LNP for SARS-CoV-1 and SARS-CoV-2 and SARS-related batCoVs (WIV-1 and SHC014). Symbols indicate individual macaques and black bars show the group geometric mean (Two-tailed Exact Wilcoxon test, n = 5 or 8 macaques).

b Serum cross-neutralization ID50 titers before (gray), after two (light blue) or after three (blue) RBD-scNP immunizations. Bars represent the group geometric mean.

c Human, bat, and pangolin SARS-related betaCoV S protein ELISA log AUC titer for plasma IgG from macaques immunized twice with RBD-scNP. ECD, ectodomain.

d Structural comparison of the epitopes of SARS-CoV-2-specific neutralizing RBD antibody (DH1041, red, PDB ID: 7LAA) and cross-neutralizing RBD antibody (DH1047, magenta, PDB ID: 7LD1). (Left) Cartoon view of Spike (green), RBD (gray), Receptor Binding Motif

(RBM, blue). (Right) Overlay of the RBDs of the two complexes from their respective cryo-EM structures.

e RBD colored by conservation within group 2b betacoronaviruses. DH1047 epitope is shown in magenta outline.

f Heatmaps displaying pairwise amino acid sequence similarity for 57 representative betaCoVs.

g, h Plasma/serum antibody blocking of S-2P binding to ACE2 (gray) and DH1047 (navy blue). **g** Kinetics of SARS-CoV-2 or batCoV-SHC014 blocking by serum from macaques immunized twice with RBD-scNP. Group mean±s.e.m. are shown (n = 5 macaques).

h Blocking activity by serum from macaques immunized twice with RBD-scNP or S-2P mRNA-LNP and humans immunized twice with Pfizer BNT162b2 or naturally infected with SARS-CoV-2. Each symbol represents an individual subject and filled bars indicate the group mean in **h**. Positivity threshold (dashed line) is greater than 20% in **g** and **h**.

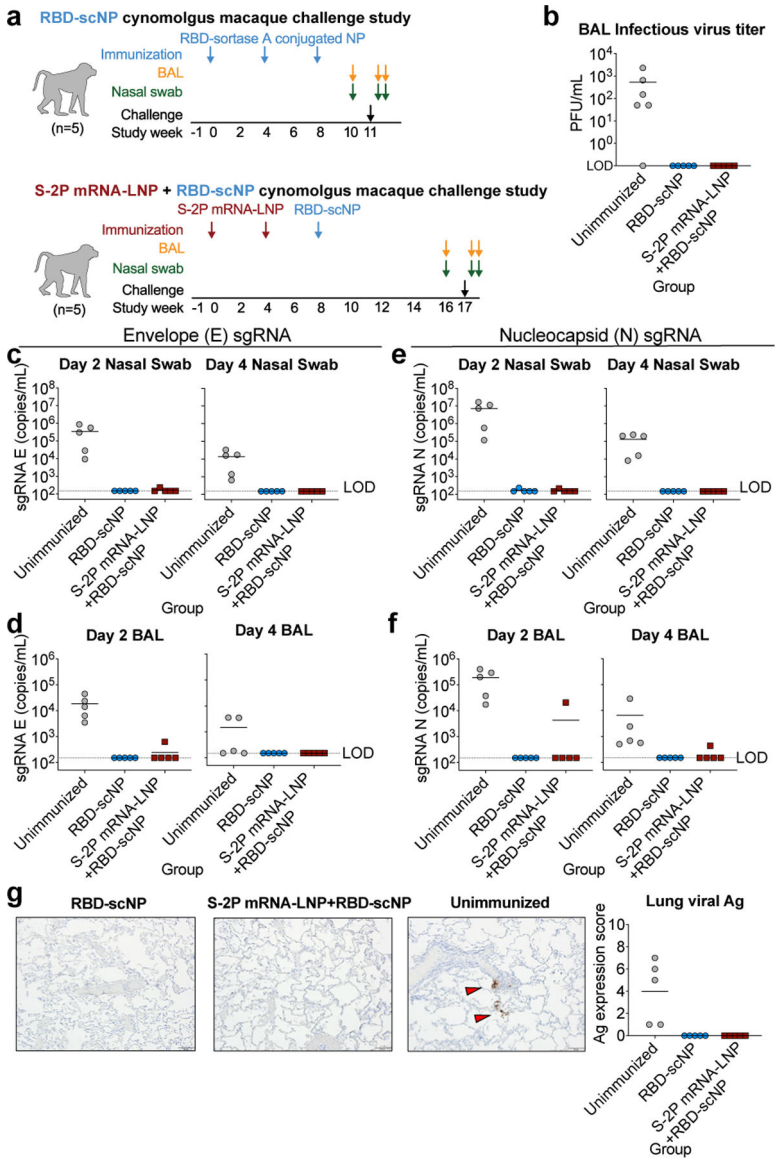

Figure 4. RBD-scNP vaccination alone or as a boost completely prevents virus replication in the upper and lower respiratory tract after intranasal and intratracheal SARS-CoV-2 challenge in nearly all macaques.

a. Macaque intranasal/intratracheal SARS-CoV-2 challenge study design. Blue and maroon arrows indicate the time points for RBD-scNP and mRNA-LNP immunizations respectively.

b Infectious virus in macaque BAL fluid two days after challenge.

c-f. Quantification of viral envelope (E) gene or nucleocapsid (N) gene subgenomic RNA (sgRNA) in unimmunized (gray) and RBD-scNP-immunized (blue), and S-2P mRNA-LNP prime/RBD-scNP boosted (burgundy) macaques. sgRNA in nasal swabs and bronchoalveolar lavage (BAL) was quantified two (left) and four (right) days after challenge. Limit of detection (LOD) for the assay is 150 copies/mL. Symbols and bars are shown as in **b**.

g Nucleocapsid immunohistochemistry of lung tissue sections seven days post challenge. (Left) A representative image from 1 macaque from each group of 5 macaques is shown.

Red arrows indicate site of antigen positivity. All images are shown at 10X magnification with 100 micron scale bars. (Right) Quantification of antigen positivity. In each panel symbols represent individual macaques with the group mean shown as a black horizontal bar.